The Dissertation Committee for Fan Tu Certifies that this is the approved version of the following dissertation:

SYSTEMATIC ANALYSIS OF RFX2 TARGET GENES IN VERTEBRATE MULTICILIATED CELLS

Committee:

John B Wallingford, Supervisor

Edward M Marcotte

Kyle M Miller

Theresa O'Halloran

Tanya T Paull

SYSTEMATIC ANALYSIS OF RFX2 TARGET GENES IN VERTEBRATE MULTICILIATED CELLS

by

Fan Tu

Dissertation

Presented to the Faculty of the Graduate School of

The University of Texas at Austin

in Partial Fulfillment

of the Requirements

for the Degree of

Doctor of Philosophy

The University of Texas at Austin

December 2017

Acknowledgements

I want to thank my adviser, Dr. John Wallingford, for his guidance over the past six years. He did not only teach me the methods on how to perform scientific research work but also he is a great example of a critic and creative scientist. I also want to thank my committee members: Dr. Edward M Marcotte, Dr. Kyle M Miller, Dr. Theresa O'Halloran and Dr. Tanya T Paull for their patience and valuable advices on my research plans and career development. I would like to thank Mei-I Chung and Asako Shindo for their guidance when I joined the lab. I am also so lucky to have Jakub Sedzinski as my great friend and collaborator for the past years. I thank all the other Wallingford lab members for their kindness and help. Finally, I am really grateful for the unlimited and unconditional support and love from my wife, my parents, and the whole family, without which I would not achieve anything in my life.

SYSTEMATIC ANALYSIS OF RFX2 TARGET GENES IN VERTEBRATE MULTICILIATED CELLS

Fan Tu, Ph.D.

The University of Texas at Austin, 2017

Supervisor: John Wallingford

Multiciliated cells (MCCs) drive directional fluid flow in diverse tubular organs and are essential for development and homeostasis of the vertebrate central nervous system, airway, and reproductive tracts. These cells are characterized by dozens or hundreds of long, motile cilia that beat in a coordinated and polarized manner. In recent years, genomic studies have not only elucidated the transcriptional hierarchy for MCC specification, but also identified myriad new proteins that govern MCC ciliogenesis, cilia beating, or cilia polarization. Interestingly, this burst of genomic data has also highlighted the obvious importance of the "ignorome," that large fraction of vertebrate genes that remain only poorly characterized. Understanding the function of novel proteins with little prior history of study presents a special challenge, especially when faced with large numbers of such proteins. Here, we explored the MCC ignorome by defining the subcellular localization of 260 poorly defined proteins in vertebrate MCCs in vivo. Based on this localization data, we selected some targets of MCC ignorome for further functional studies because they could possibly play key roles in the regulation of ciliogenesis. We characterized Myo5c as the motor for basal body apical migration,

Arhgef18 as the RhoA signaling activator at the basal bodies, and Dennd2b as a regulator of actin network formation and ciliogenesis. All of these findings have deepened our understanding about molecular mechanisms of related cellular process. This study exemplifies the power of high content protein localization screening as the bridging step between large-scale omics data and functional study of specific proteins.

Table of Contents

List of Tables

List of Figures

Chapter 1: General introduction

1.1 MULTICILIATED CELLS ARE WIDELY DISTRIBUTED IN HUMAN BODIES AND PLAY VITAL PHYSIOLOGIC FUNCTIONS IN DIFFERENT ORGANS AND TISSUES.

Multiciliated cells (MCCs) are a specific type of epithelial cell that have dozens or hundreds of cilia extending from the cell surface[1]. Each cilium is a microtubule based and membrane enveloped small protrusion. MCCs play different functions in different organs and tissues by generating directional fluid flow through synchronized and coordinated cilia beating[2-5]. For example, ependymal cells are multiciliated epithelial cells that line the walls of the ventricles in the adult brain, circulating cerebrospinal fluid. Defects in ependymal cell development or functions lead to cerebrospinal fluid accumulation and expansion of ventricles, resulting in hydrocephalus[2, 5]. MCCs are also distributed on the epithelia of human upper airway, where the beating of cilia propels excess mucus and debris out of the airway.[2, 4] There is also evidence suggesting that these cells are chemosensory, and as such they are able to modulate their activity in response to environment stimulus[6]. Defects in airway MCCs lead to compromised host defense and recurrent infections of the airways[2, 4]. MCCs are also found in the oviduct of female reproductive tracts and are responsible for ova transportation. Defects in oviduct MCCs may lead to infertility[2, 3]. In all, MCCs play important physiologic functions in human bodies, and defects in these cells cause awide range of severe diseases in patients. Thus, studying the development of MCCs and the regulation of MCC functions are of great importance and may help to improve human health.

1.2 DEVELOPMENT OF MCC IS A MULTISTEP PROCESS INVOLVING DISTINCT CELLULAR BEHAVIORS.

1.2.1 MCC cell fate determination is controlled by signaling pathways and transcription factors

In *Xenopus* epithelium, MCC precursor cells differentiate from progenitor cells in the deep layer of epithelium under control of many signaling pathways and transcription factors[7, 8].

Notch signaling suppresses MCC cell fate determination. Activation of Notch signaling blocks MCC differentiation and results in more secreting cells instead[9-11]. What lies upstream of Notch signaling in MCC cell fate determination is still unknown. MiR-449 has been shown to enhance ciliogenesis through inhibition of Notch signaling by directly binding to the mRNA and reducing the transcript level of Notch activating ligand Dll1[12]. BMP signaling also suppresses ciliogenesis, but it is required for MCC intercalation, suggesting that BMP signaling plays different roles at different developmental stages of MCC[13]. Wnt signaling enhances ciliogenesis[14]. However, it is still not clear how these different signaling pathways cooperate to determine MCC cell fate.

Many transcription factors have been identified as ciliogenesis regulators. Gemc1 (Geminin coiled-coil domain-containing protein 1) is a master transcription factor required for proper ciliogenesis and is sufficient to induce ectopic ciliogenesis in nonciliated cells[15-17]. Gemc1 functions downstream of Notch signaling but upstream of Mcidas and Foxj1[15].

Foxj1 (forkhead box protein J1) is also required for ciliogenesis, however, ectopic expression of Foxj1 is only able to induce single or double cilia in each cell, indicating other factors are required for multiciliation[18, 19]. Many of Foxj1 induced genes are shown to have specific localization in ciliated cells and are required for ciliogenesis[20].

Inhibition of Notch signaling leads to activation of Mcidas (multiciliate differentiation and DNA synthesis associated cell cycle protein) expression[21]. Ectopic expression of Mcidas is able to induce multiciliation[21]. Mcidas does not activate transcription directly but binds to E2F4/5 transcription factors as a complex to activate the ciliogenesis program[22].

The RFX (regulatory factor X) family of transcription factors are broadly required for ciliogenesis in different organisms and different tissues[7, 23, 24]. Rfx2 is highly and specifically expressed in *Xenopus* MCCs and is required for MCC development but not for MCC cell fate determination, and Rfx2 is not sufficient to induce ciliogenesis ectopically in other cells[24].

The relationships between these transcription factors are still unclear. Gemc1 is on the top of this transcriptional controlling network[15], because it is able to activate expression of Mcidas and Foxj1, which are at the same level downstream of Gemc1[15]. Rfx2 is more likely an enhancer of ciliogenesis[7, 25], which is further supported by the finding that Rfx2 and Foxj1 forms a complex that binds at the promoters of ciliary genes and activate their expression[26]. Moreover, all of these transcription factors control very different profiles of target genes. However, only a very small fraction of target genes are shared by these transcription factors. Thus, it is of great importance to study the functions

of the target genes of these transcription factors to understand more fully about their roles in regulating the development of MCCs.

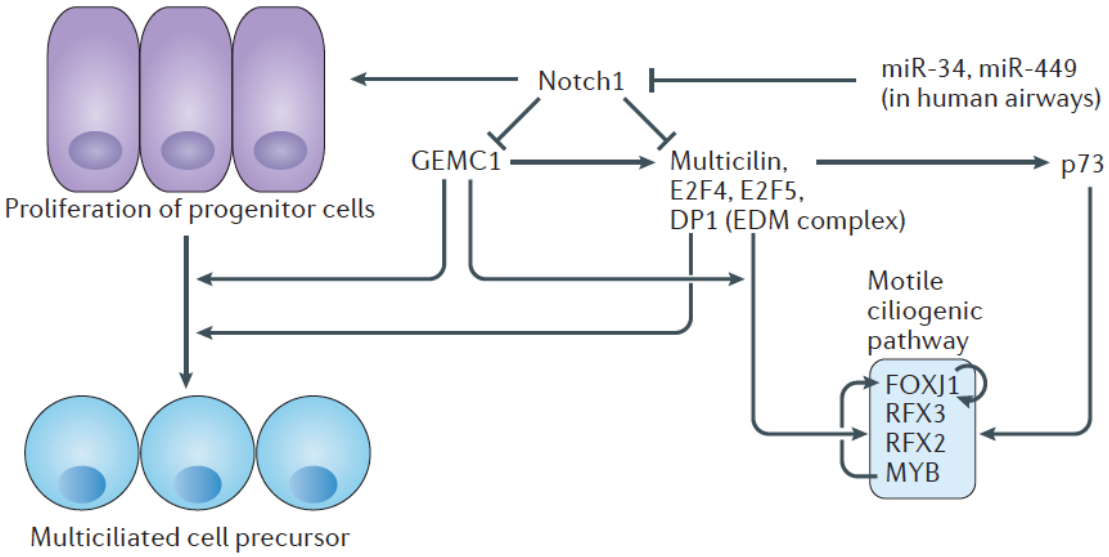

Figure 1.1 Transcriptional regulation of MCC

The network of different transcription factors controlling MCC differentiation. Figure adapted from Spassky and Meunier, 2017[2]

1.2.2 MCC precursor cells intercalate through cell junctions

MCCs are born from progenitor cells basal to the epithelium. After the cell fate is determined, MCC precursor cells migrate apically from the deeper layer of the epithelium to the surface layer through tricellular junctions, in a process called cell radial intercalation[9, 27]. The detailed molecular mechanism controlling MCC precursor cell intercalation is still unknown[28, 29], however evidence suggests that this process is tightly regulated on different molecular levels. Knocking down Rfx2 leads to multiple defects of MCC development including cell intercalation defects[25]. Dystroglycan is expressed in the

inner layer of epithelia, and is required for MCC differentiation and intercalation[30]. Many other proteins have been shown to be enriched at the apical surface of the intercalating cell, such as Rab11[31], Par3 [32]and Vangl2[33]. These three proteins are required for proper intercalation of MCC, possibly because they are required for establishing the polarity of the cell.

1.2.3 MCC precursor cells integrate into the existing epithelia through apical emergence

When MCC precursor cells reach the surface of the apical layer of epithelia, they expand their cell surfaces while integrating into the existing epithelia, in a process termed as apical emergence[34]. Apical emergence is a cell behavior conserved in different self-renewing tissues and organs, however the dynamics and molecular mechanisms of this process have not been revealed until recently. Slit2 is well studied for its role in regulating neuron cell migration. Chung et al., found it was an Rfx2 direct target gene that was required for MCC precursor cell apical emergence. With Slit2 knock down, MCC precursor cells were able to reach the surface of the epithelia but failed to expand their cell surfaces[25]. By long time-lapse in vivo live imaging and biophysical modeling, Sedzinski et al showed that the apical emergence was mainly driven by the pushing force generated by actin polymerization[34]. The detailed molecular mechanisms that demonstrate how the actin dynamics are regulated during the process of apical emergence are still unknown.

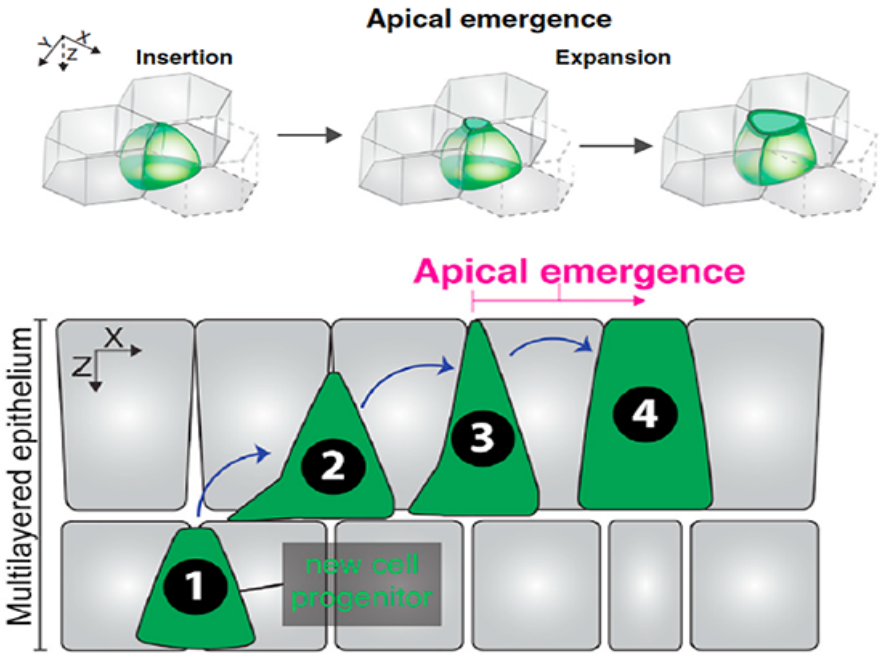

Figure 1.2 MCC intercalation and apical emergence

1.2.4 Transition fibers anchor basal bodies to cell membrane and recruit other proteins for ciliary functions

The transition fibers are specialized distal appendages, which anchor basal bodies to the cell membrane. Between each of these transition fibers, there is a gap about 60nm that is large enough for many macromolecules to pass through[35]. Many proteins have been identified as transition fiber components, such as Cep83, Fbf1, Cep89, Cep164 and Sclt1[36]. Some evidence suggests that there are hierarchy relationships between these transition fiber proteins' localizations. For example, Cep83 is required for localization of

Fbf1, Cep89, and Cep164; Sclt1 is required for Fbf1 and Cep164. All of these transition fiber proteins are required for ciliogenesis[36, 37].

Since the gaps between transition fibers are relatively large, the major functions of transition fibers are basal body docking and recruiting other proteins to facilitate ciliogenesis. For example, knocking down of Cep83 leads to failure of basal body docking and defects of ciliogenesis[37]. Cep164 is required to recruit Ttbk2, which is essential for Ccp110 removal to initiate ciliogenesis. Cep164 is also able to recruit Inpp5e, which is required for ciliogenesis and ciliary trafficking[38]. Some evidence also suggests that transition fiber proteins may directly contact with IFT proteins. For example, FBF1 directly binds to IFT54, an IFT-B component, and regulates its entry into cilia[39].

1.2.5 Basal body planar polarity and cilia beating

The cilia of each MCC beat in a synchronized and coordinated way, and the polarity of ciliary beating is mostly determined by planar polarity of basal body orientations.

Both PCP core proteins and PCP effectors have been shown to regulate basal body orientation polarity[40, 41]. Park et al. showed that the PCP core protein, Dishevelled, localized asymmetrically at basal bodies. Further, that Dishevelled was required for both basal body docking and polarity establishment, probably through regulating RhoA signaling activation at basal bodies[40]. Butler and Wallingford showed that Prikle2 localized asymmetrically to the ventroposterior side of the MCC cortex membrane. This asymmetric localization pattern was established progressively as MCCs matured, and it

was required for basal body polarity.[41] Some proteins control basal body polarity indirectly through regulating PCP proteins[42]. For example, c21orf59/kurly bound to Dishevelled and was required for cilia polarized beating both in *Xenopus* and *Zebrafish*[42]. The molecular players downstream of PCP signaling are still unknown, though evidence suggests that polarized cytoskeleton networks are involved in this process[43].

It is believed that basal body polarity is established by connecting the striated rootlets to the basal feet of the nearby basal bodies, and microtubule polarity is also involved in this process[43, 44]. Werner et al. showed that the subapical actin network was responsible for connecting basal bodies and rootlets. Disrupting the subapical actin network led to severe basal body spacing defects[44]. Some basal foot localizing proteins have been identified and shown to be required for basal body polarity establishment[45, 46]. Odf2 localized to basal feet and knocking out Odf2 led to loss of basal feet and disrupted basal body polarities in mice tracheal cells, probably because of the failure of connecting basal feet to cytoskeleton networks and rootlets[45]. This was further confirmed by the finding that Zeta-tubulin, the sixth and final member of the tubulin superfamily, localized specifically to basal feet and was required for subapical actin foci formation and basal body orientation polarity[46]. So far, the detailed mechanisms about how cytoskeleton and basal body positions are coordinated and modulated are still unknown.

1.3 ACTIN REGULATES MULTIPLE CILIARY PROCESSES

1.3.1 Actin is involved in basal body migration and docking

After basal bodies are generated from the deuterosomes deep in cytosol, they migrate apically to the surface of MCCs[47, 48]. Early immunostaining and EM studies showed that actin and myosin were enriched around basal bodies during their apical migration[48]. Treatment with actin depolarizing drugs disrupted basal body migration[49, 50]. PCP protein Dishevelled and activation of RhoA signaling were both required for basal body migration[40, 50], possibly through activating myosin and regulating actin dynamics in situ around the basal bodies. One interesting study from the Skourides lab showed that the focal adhesion protein Fak connected the basal body to actin networks[51]. Many other proteins were also required for basal body docking, such as, nucleotide binding protein1(xNubp1)[52], deubiquitinating enzyme CYLD[53], Rac1 regulator ELMO, Ezrin[54], Nphp4, Daam1[55], Flattop[56], Chibby[57], and FAM92[58]. Defects in the proper functions of these proteins, they all led to severe actin network defects, basal body docking failure and ciliogenesis defects, though the exact mechanism details are still unknown. We still do not know how actin is involved in basal body migration nor what the molecular basis of basal body transportation system is.

1.3.2 Apical cortex actin networks

Actin forms tightly regulated network structures at the apical surface of the MCC cortex. In the late 1980s, by EM studies, researchers found that actin and microtubules were enriched around basal bodies, and basal feet were connected to striated rootlets through these cytoskeletal filaments[48, 49, 59]. These findings were later confirmed by

immunostaining and confocal imaging experiments showing that the apical actin networks were composed of two layers of actin structures with different features and functions[44, 60, 61]. The apical layer formed the lattice structure around the basal bodies possibly responsible for anchoring the basal body to the actin network. This was supported by the finding that the focal adhesion complex protein Fak connected basal body to the actin lattice[51]. The subapical actin showed the foci pattern, and these foci were the places where the ends of rootlets were connected to basal feet of nearby basal bodies by actin filament. The subapical actin foci were required for basal body spacing and orientation polarity[44, 51, 59]. For example, treatment with low concentration of Cytochalasin D disrupted the subapical actin foci only, and this treatment led to disrupted basal body spacing patterns with less regulated distance between nearby basal bodies, with some of the basal bodies even clamped into chains[44]. So far, we still know almost nothing about the molecular mechanisms regulating the formation of these actin networks.

1.3.3 Actin and ciliogenesis

Besides regulating MCCs by apical network structures, actin seems to be specifically required for ciliogenesis[62, 63]. Many studies have shown that actin was required for BB docking, thus indirectly regulating ciliogenesis (this part is covered in basal body docking section). However, more and more evidence suggested that actin was able to modulate ciliogenesis directly. For example, treating the cells with Cytochalasin D increased ciliation rates and led to longer cilium lengths[64]. Cytochalasin D treatment was even able to partially rescue the ciliogenesis defects in IFT88 mutant cells[64].

Additionally, the actin regulators Limk2 and TESK1 repressed ciliogenesis, possibly through regulating the Yap signaling pathway[63]. Recently, a study found that many actin binding proteins actually localized inside the cilium[65]. Thus, it is of great interest and importance to study how actin regulation is linked to ciliogenesis.

1.4 Ccp110 is a key regulator of ciliogenesis

Centrosomal protein 110(Ccp110), was found as a novel CDK substrate, which localized to centrosome and was required for centrosome duplication[66]. Ccp110 was shown to be a repressor of ciliogenesis, because depletion of Ccp110 led to aberrant formation of cilia from the centrioles inside the cytoplasm[67, 68]. The reduction of Ccp110 has been used frequently as a reliable marker for ciliogenesis initiation[68]. Many Ccp110 binding proteins have been identified and characterized so far[69]. For example, Cep290 binds to Ccp110, and itis able to recruit Rab8, which is required for ciliogenesis[68]. Kif24 binds to Ccp110 and is able to depolymerize microtubules at the centriole to regulate ciliogenesis[70].

Many studies focus on studying the mechanisms on how Ccp110 is removed from the centrosomes before ciliogenesis, and they have identified some proteins involved in this process. Cyclin F binds to Ccp110 and catalyzes ubiquitination of Ccp110 through the SCF (Skp1-Cul1-F-box protein) ubiquitin ligase complex, and the ubiquitinated Ccp110 will be degraded by proteasomes. Tau tubulin kinase 2 (TTBK2) is also required for Ccp110 removal through unknown mechanism[71]. On the other hand, some proteins are able to stabilize Ccp110 protein stability. For example, USP33 binds to Ccp110 and

leads to its deubiquitination and stabilization at centrosomes[72]. Interestingly, some microRNAs are able to regulate ciliogenesis by controlling Ccp110 transcript levels. For example, miR-34/449 miRNAs bind to 3' UTR of Ccp110 and lead to the decrease of Ccp110 level to facilitate formation of cilia[73].

Recently, more and more evidence suggests that Ccp110 is also required for the proper formation of cilia, because the removal of Ccp110 prematurely leads to defective cilia. For example, knocking out of Ccp110 in mice led to all kinds of developmental defects caused by defective cilia structures and disrupted Shh signaling[74]. Another paper showed that knocking down Ccp110 in *Xenopus* MCCs resulted in basal body docking defects, probably because of the failure to recruit Fak to the basal bodies[75]. It is now believed that Ccp110 levels need to be properly regulated through the whole process of ciliogenesis. At the early stage, Ccp110 blocks aberrant ciliogenesis and functions as a protective cap at the centrosome, meanwhile, Ccp110 recruits binding partners that facilitate basal body migration. When the basal bodies are ready for ciliogenesis, Ccp110 recruits proteins required for basal body priming and Ccp110 removal. At last, Ccp110 is removed and ciliogenesis begins[69, 74, 75]. The detailed mechanisms regulating the profiles of Ccp110 binding proteins and Ccp110 protein levels at basal bodies still remain to be illustrated.

1.5 SYSTEMATIC STUDIES ON CILIOGENESIS

Since ciliogenesis requires the cooperation of different cellular machineries, many systematic studies have focused on identifying regulators of ciliogenesis and ciliary

functions have been performed so far[76-80]. Though most of these studies focused on primary cilia, the similar molecular mechanisms may apply to MCCs too.

RNAi screening is a powerful loss of function approach, and some papers have reported using RNAi to screen for ciliogenesis regulators[78, 81]. Kim et al. screened 7784 therapeutically relevant genes in human cells and identified 36 positive and 13 negative ciliogenesis modulators. Based on their screening results, they found that actin dynamic and endocytic recycling were tightly coupled with ciliogenesis[64]. Another study screened 19059 genes in mouse inner medullary collecting duct (mIMCD3) ciliated cell line and identified 112 ciliogenesis regulator candidates[78]. A morpholino screen in Zebrafish was also reported. Austin-Tse et al. screened 10 genes, whose protein products had been identified previously in cilium proteome, and identified CCDC65 and C21orf59 as genes causing primary ciliary dyskinesia[82].

The transcriptome of ciliated cells contains useful information for understanding ciliogenesis and ciliary functions[83, 84]. For example, by microarray analysis of ciliated mice trachea epithelia cells, Hoh et al. identified 649 genes upregulated early, when most cells were forming basal bodies, and 73 genes upregulated late, when most cells were fully ciliated. They further characterized three genes that produced proteins localized to the centrosome and cilia [83]. Similarly, by using the whole-organism RNA-seq libraries, Jensen et al. discovered that a cluster of 185 genes that shared signature expression profile to that of known ciliary genes, and they further characterized Rab28 as a novel regulator of the BBSome and IFT[84].

Many extensive proteomic studies have been performed to understand the protein composition of ciliary structures[77, 79]. For example, Gupta et al. used proximity-dependent biotinylation (BioID) to map the proteins present at the centrosome-cilium interface. With 58 bait proteins, they generated a protein interaction map with over 7000 interactions[77]. Similarly, Boldt et al. used systematic tandem affinity purifications, and with 217 tagged human ciliary proteins, they were able to generate a protein-protein interaction map with 1,319 proteins, 4,905 interactions and 52 complex[79].

Several imaging based approaches have been reported for identifying novel ciliary genes[20, 85, 86]. Hayes et al. used an in situ hybridization-based approach to analyze the gene expression patterns in *Xenopus* epithelia, because the ciliary genes would show the distinct salt and pepper pattern. They were able to identify over 30 ciliary genes, and most them have been shown to be involved in ciliary processes so far[85]. Choksi et al. screened protein localizations of 50 Foxj1 controlling genes in Zebrafish ciliated cells, and further characterized their functions in ciliated cells by morpholino knock down experiments[20].

Moreover, though all of these large-scale or high content studies were able to identify many promising novel ciliogenesis and ciliary function modulator candidates, it is still a great challenge to study the functions of these candidates systematically. This is one of the major reasons why we still know very little about the detailed molecular mechanisms of most ciliary processes.

1.6 *XENOPUS* EPITHELIUM IS A POWERFUL MODEL FOR MCC STUDIES.

The *Xenopus* epithelium is a powerful model for MCC studies for the following reasons. On one hand, *Xenopus* and human MCCs share many key features. For example, they have similar morphology and cellular components; the cilia beating generates directional fluid flow on the surface of epithelia; the development of MCC and regulation of functional activities are under the control of similar signaling pathways and hormone regulations. On the other hand, *Xenopus* MCCs have some special features to be favored for MCC studies. First, unlike the human MCCs that line inside of human bodies, *Xenopus* MCCs develop on the surface of tadpole epithelia, thus they are easily accessible for many different manipulations, such as live imaging and drug treatments. Second, the development of *Xenopus* MCCs only takes less than 48 hours, which is much shorter than the development of human MCCs. The shorter developmental time not only speeds up research process but also enables the use of long time-lapse imaging to understand the dynamic cellular behaviors of MCCs. For example, Sedzinski et al. performed live imaging on the whole process of MCC apical emergence, which took about 2 hours in *Xenopus*. With this kind of data, they were able to study the whole process with biophysical modeling methods, and test the effects of different drug treatments on different stages of apical emergence. Likewise, both *Xenopus* and human beings are vertebrates, so they may share higher homology than other nonvertebrate model organisms such as *Chlamydomonas* and *C.elegans*. At last, many molecular tools and methods have already been developed for MCC studies in *Xenopus*. For example, it is quite straightforward and robust to use morpholino for loss of function studies in *Xenopus*. (morpholino is a synthesized RNA oligo that binds to the RNA splicing sites to reduce normal transcripts or binds to translation start site to block protein synthesis.)

Another case is that the Kintner lab developed the drug inducible multicilin activation system, which enables inducing multiciliation of goblet cells by drug treatment. With all of these great features, much progress on understanding development of MCCs has been achieved by using *Xenopus* as a model for MCC studies.

Chapter 2: High-content protein localization screening in vivo identified subcellular localization of novel proteins in MCCs

2.1 INTRODUCTION

Rfx2 is an Rfx (regulatory factor X) family transcription factor which is highly and specifically expressed in MCCs. Rfx2 is required for proper ciliogenesis and ciliary functions[24, 87]. Direct target genes of Rfx2 have been identified by RNA-seq and Chip-seq[25]. Out of these 911 direct targets, about 150 of them have been reported to be ciliary genes. By Humannet probability prediction and functional analysis, some Rfx2 targets have been identified as novel regulators of ciliogenesis or ciliary functions, such as IFT trafficking and cilia beating[25]. However, the functions of the majority of Rfx2 target genes are still unknown.

Systematically studying the functions of large lists of genes is still challenging. Most previous studies have used the loss of function screening method, however these approaches are not easily applicable nor practical for vertebrate animal studies. Other studies have used high content protein localization screening approaches to address this problem[20, 88]. MCCs are very compartmented and composed of structures of different functions. For example, the basal body is the foundation of the cilium and is important for axoneme growth and recruiting ciliogenesis proteins, and transition zone proteins are required for selective substrate filtration[25]. Thus, the localizations of the proteins in MCCs may provide important information to guide us in understanding the functions of these proteins in MCCs.

2.2 RESULTS

2.2.1 Systematic preparations of screening vectors were achieved by combining Human ORFeome collection and Gateway cloning system

To identify the localizations of uncharacterized or poorly characterized Rfx2 target genes, we combined the Human ORFeome collection and the Gateway cloning system to systematically generate the vectors required for localization screens. The open reading frames of interesting Rfx2 target genes were inserted by Gateway reactions into destination vectors containing N-terminal or C-terminal fluorescent protein tags as well as an MCC-specific promoter. We then injected each of these 260 plasmids directly into blastula stage *Xenopus* embryos and observed the localization of the fluorescently tagged proteins in MCCs by confocal microscopy. All plasmids were co-expressed with membrane-BFP to visualize the membrane structures, thus ensuring that localization data reported here is for MCCs.

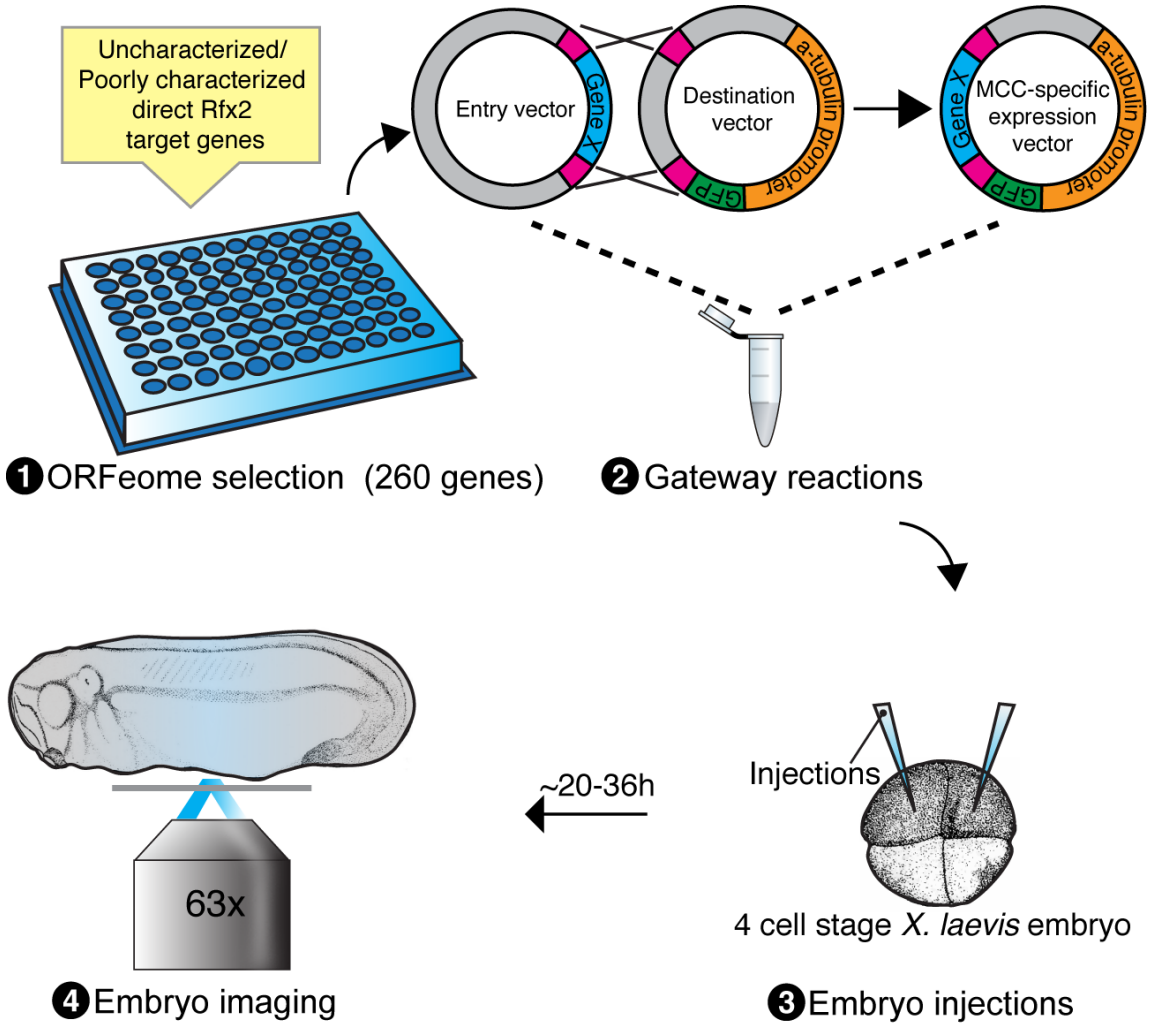

Figure 2.1 Pipeline of high content protein localization screening

Briefly, using GATEWAY cloning reactions, 260 human open reading frames (ORFs) corresponding to Rfx2 direct target genes were inserted into destination vectors containing N-terminal or C-terminal fluorescent tags along with a MCC specific α-tubulin promoter. All resulting plasmids were then sequenced from both ends. Circular plasmid (~50pg) was then injected into *Xenopus laevis* embryos at the 4-cell stage as described. Plasmids were injected along with membrane-BFP to visualize axonemes, thus ensuring that the localization reported was for MCCs.

2.2.2 The protein localization screen identified many Rfx2 targets encoded proteins localized to specific subcellular structures

Of the 260 candidates tested, 235 of them were effectively expressed based on GFP or RFP fluorescence, and 199 of them were detected with discrete localization patterns in MCCs

Consistent with the well-established role for Rfx2 in regulating ciliogenesis and ciliary functions, some of screened proteins localized to axonemes and/or the basal bodies. For example, Efhc2 is a gene related to Idiopathic generalized epilepsy, and it localized to axonemes, similar to that of Efhc1. Tctn3 is supposed to be a transition zone protein, and it localized to basal bodies. Moreover, some totally unstudied proteins also showed localization to basal bodies and axonemes suggesting they might have important ciliary roles. For example, Fam166b and Ccdc33 are essentially unstudied and were found strongly restricted to the ciliary axoneme. Mtmr11 and Ankrd45 are similarly uncharacterized and were found specifically at basal bodies.

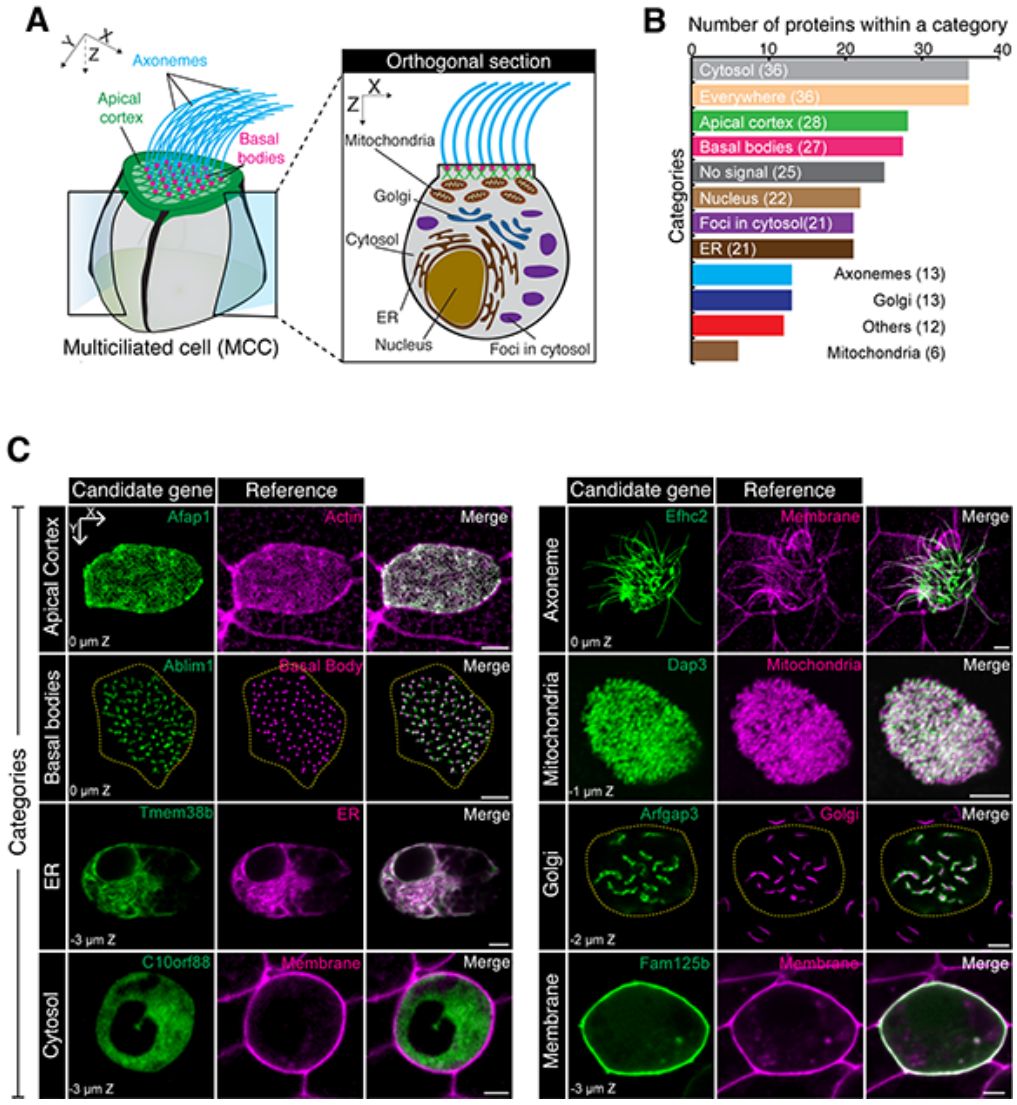

Figure 2.2 The screen identified 199 Rfx2 targets localize to specific MCC subcellular structures

(A) Schematics of MCC subcellular structures, indicating the major distinct subcellular structures identified in our screen. **(B)** Summary of screening results. Out of 260 candidates, 199 showed detectable signal localized to distinct subcellular structures categorized on a histogram. **(C)** Representative localizations of screened Rfx2 targets. Left columns, expression patterns of selected genes; middle columns, expression patterns of reference genes. Afap1 localizes to actin cortex (marked by LifeAct-RFP), Efhc2 to axonemes (marked by CAAX-RFP), Ablim1 to basal bodies (marked by Centrin4-BFP), Dap3 to mitochondria (marked by mito-RFP), Tmem38b to ER (marked by Cal-BFP-knockdownEL), Arfgap3 to Golgi apparatus (marked by GalT-RFP), C10orf88 to cytosol, and Fam125b to basolateral membrane (marked by CAAX-RFP). Number at the bottom-left corner indicates Z-plane position in reference to the apical domain (0 µm Z). Scale bar, 5µm. Yellow dotted line outlines the cell boundary of a MCC

One of biggest localization groups is the apical cortex group, however, almost none of them have been studied for their functions in the MCCs yet. Many of these proteins are actin related, such as Afap1, Fmn1, Myo5c, Palld, Pls3, Dennd2b, and so on. The discreet apical actin networks on the cell surface of MCCS have been shown to play key roles in regulating ciliogenesis and ciliary functions. However, very little is known about the molecular mechanisms regulating formation and functions of these apical actin network structures. These proteins' localization patterns suggest they may be involved with these actin network related processes.

Curiously, the majority of screened Rfx2 targets did not localize to well defined ciliary structures, but rather to other cellular organelles or other subcellular structures, including nucleus, Golgi apparatus, endoplasmic reticulum, cytoskeletal networks, and foci like structures. Though these subcellular structures are not specific to multiciliated cells, these proteins may still perform MCC specific functions for the following reasons. First, all of these genes are Rfx2 direct target, and Rfx2 is highly and specifically expressed in MCCs, so these genes may be specifically turned on in MCCs. This was supported by the evidence demonstrated that some of these genes showed MCC specific expression patterns in *in situ* hybridization experiments. Second, some previous studies reported that some proteins localized to these noncliliary structures but were also required for ciliogenesis. For example, Xpnpep3 localized to mitochondria, and mutation in this gene led to a Nephronophthisis-like disease, because Xpnpep3's peptide cleavage activity was required for processing the substrates required for ciliogenesis. Another protein,

Pih1d3, was shown to be required for axonemal dynein assembly, but localized to the Golgi apparatus. And last, considering that MCCs are very distinct from other types of cells in cell morphology and cell structures, it is reasonable that some ciliated cell specific molecular machineries may specifically exist in the cytoplasm of MCCs. During ciliogenesis, hundreds of cilia are built at the same time. This process requires large amounts of substrates synthesized and transported in a very short time, so the whole cell, including these ciliary and nonciliary structures needs to tightly coordinated to meet the needs. Thus, identification of ciliary proteins localizing to nonciliary structures may provide functional insights for studying how different cellular machineries cooperate to regulate ciliogenesis and ciliary functions.

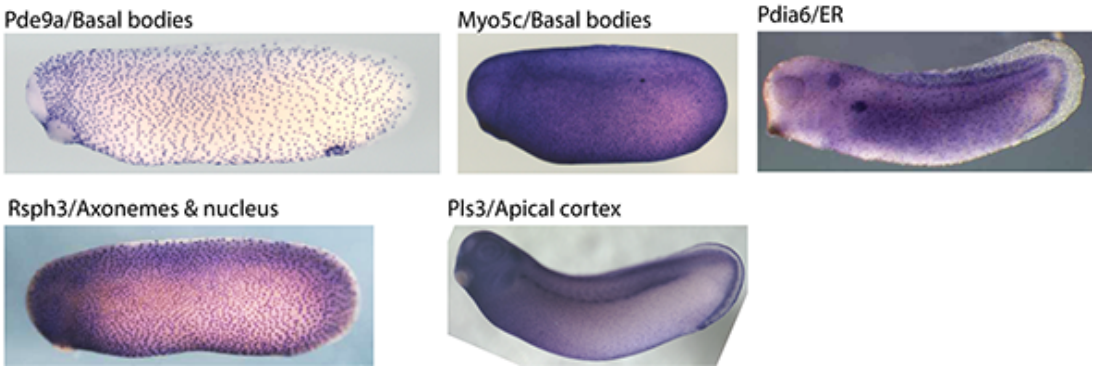

Figure 2.3 In situ data of some selected Rfx2 targets

2.2.2 The subcellular localization data of disease related proteins may help understanding the etiology of these diseases

For the genes screened in this study, more than 40 of them have been reported as diseases related genes. Some of them are known to cause ciliopathies, such as Armc4, Kurly, Ccdc65, Rsph3, Tctn3, and Wdr60. However, we know nothing about their molecular functions. Our localization data may help understand their functions in ciliary processed. For example, Ccdc65 mutations cause primary ciliary dyskinesia and loss of axonemal dyneins[82, 89]. We found Ccdc65 localized to the basal bodies and foci in cytosol, and is possibly involved in dynein arm transportation.

Another group of genes of particular interest are Cdc14A[90], Lrtomt[91], and Tprn[92]. Mutations of these genes cause deafness in patients. Considering the similarity between MCCs and hair-cell stereocilia, their localization patterns might be conserved between these two cell types. This also suggests that studies in MCCs may help us understand some other cell types too.

Finally, we also found many genes that cause some diseases which are not obviously related to cilia. For example, Avpr2 localized to the ER, and its mutation led to nephrogenic diabetes insipidus[93], resulted from kidney dysfunctions. Considering the well-established role of cilia in regulating kidney functions, it is reasonable to suspect that the mutation of Avpr2 leads to cilia defects in kidney, and then the malfunctions of kidney lead to nephrogenic diabetes insipidus, though proper functional studies are required to test this assumption.

2.3 DISCUSSION

In summary, this screen identified the subcellular localizations of nearly 200 proteins encoded by direct Rfx2 target genes in MCCs. These proteins localized to both ciliary and nonciliary structures. This localization data may serve as a clue for understanding the protein functions in MCCs.

Note that only 13 proteins in our screen localized to the axonemes, which is quite surprising because proteomic studies have shown that many proteins were identified as axonemal proteins. On the contrary, many proteins localized to basal bodies and apical cortex. It is possible that Rfx2 controls only very few axonemal protein genes, but it is also possibly due to axonemal proteins being more sensitive to fluorescence proteins tags and fewer of them could localize to the axoneme correctly.

In addition, the identification of proteins localized to nonciliary structures may help to understand how different cellular machineries cooperate to regulate ciliogenesis and ciliary functions.

Further, we identified the subcellular localizations of more than 40 of Rfx2 targets that are human disease related. The localization data may provide valuable information to help understand the etiology of these diseases.

Chapter 3: Myo5c functions as the motor for basal body apical migration

3.1 INTRODUCTION

Newly generated basal bodies migrate apically from deuterosomes to the cell surface[1, 2] of MCCs. Much evidence has been accumulated to suggest that actin is playing key roles in regulation of this process. Enriched actin and myosin were detected around the basal bodies during their apical migration[2], and treatment with an actin depolarizing drug disrupted basal body migration[3, 4]. However, the exact mechanisms of how actin and actin related processes are regulating basal body apical migration are still largely unknown.

3.2 RESULTS

3.2.1 Basal bodies migrate apically along specific actin cables

First, we tried to determine how actin structures are involved in basal body apical migration by the staining of actin in sectioned samples from embryos at early stages when basal bodies started to migrate, and the late stages when all basal bodies docked into the ciliary membrane.

At the early stage (Stage 18), the Phalloidin stained actin cables extending from the cell center to the surface of the MCCs. Along with the generation of more basal bodies, more actin cables were detected in the samples from the later stage (Stage 19) embryos too. It was quite striking that these actin cables were only detected in the MCCs but not in the other cells types in the same epithelium such as goblet cells. These cables disappeared

when all of the basal bodies docked to the surface of the MCCs. These results suggest that the actin cables detected in the MCCs were specialized structures generated specifically for basal body apical migration.

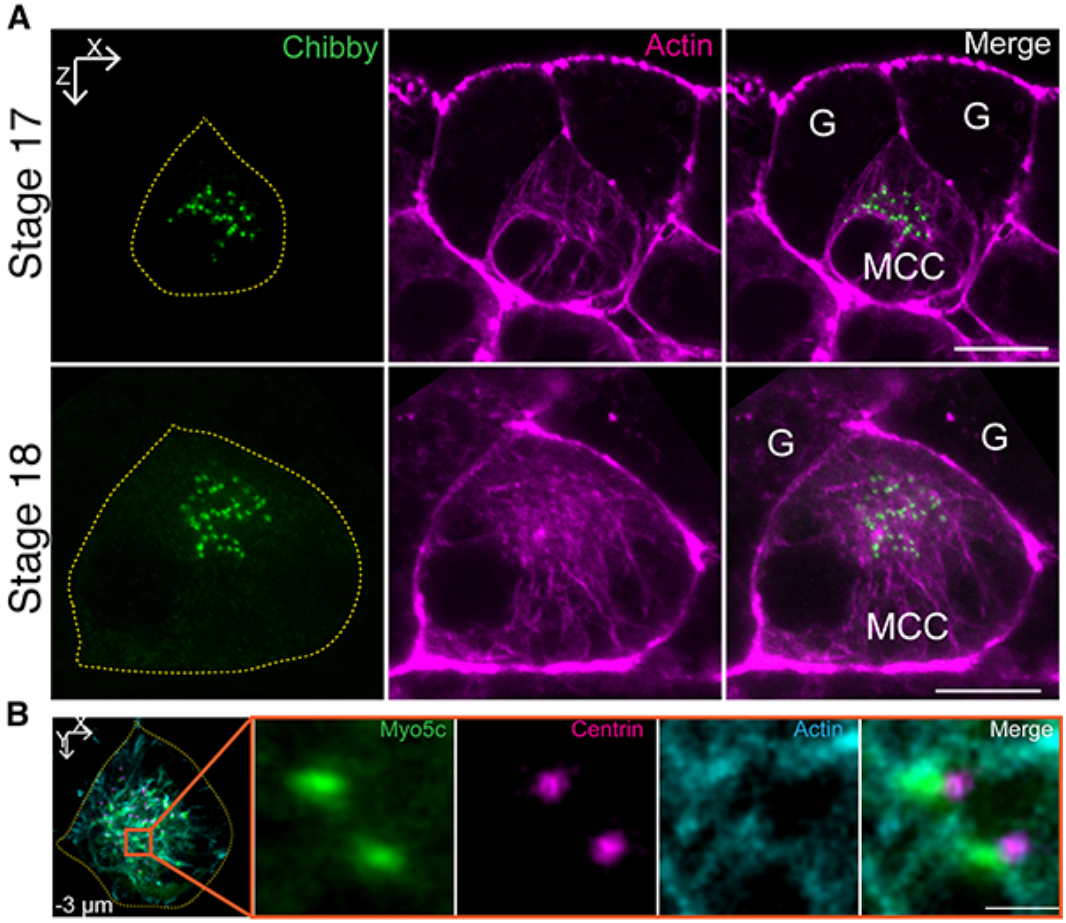

Figure 3.1 Basal bodies migrate along actin cables

(A) Sagittal sections of early stage intercalating MCCs showed basal bodies (Chibby-GFP, green) migrating along actin cables (Phalloidin, magenta) to the apical surface of MCC. G, goblet cell. Scale bar, 5µm. **(B)** Myo5c-GFP (green) localized in a proximity to basal bodies (Centrin4-RFP, magenta) and aligned with actin cables (LifeAct-BFP, cyan). Images were taken at stage 19, 3 µm below the apical surface of MCC (outlined by a yellow dotted line). Orange square, zoomed region. Scale bar, 1 µm.

3.2.2 Myo5c is required for basal body migration

With the discovery that basal bodies migrated apically along these specific actin cables, we wondered what might be the motor for this process. In our protein localization screen, we found that Myo5c, a nonconventional Myosin[5], localized to basal bodies during their apical migration. Myo5c showed an elongated droplet shape (possibly the shape of striated rootlet) connecting to basal bodies at one end and migrating along the actin cables at the other end.

Since Myo5c was known to control actin-based movements of intracellular cargoes and organelles, such as melanosomes and secretory vesicles[6, 7], we tested whether Myo5C might function as the motor for basal body apical migration.

Myo5c is composed of the N-terminal myosin motor domain and the C-terminal cargo binding domain[5]. The dominant negative form of Myo5c, in which the N-terminal myosin domain is truncated but cargo-binding domain remains intact, is widely used to study its cellular functions[6, 7]. We also used the α -tubulin promoter to drive the expression of dominant negative Myo5c to specifically study its function in MCCs.

The dominant negative Myo5c still bound to the basal bodies as expected, and the overexpression of it led to severe basal body docking defects. As the results showed, compared with control cells in which over 95 percent of basal bodies docked well on the surface, Myo5 DN overexpressed cells had severe basal body docking defects with over 75 percent of the basal bodies failed to reach the surface.

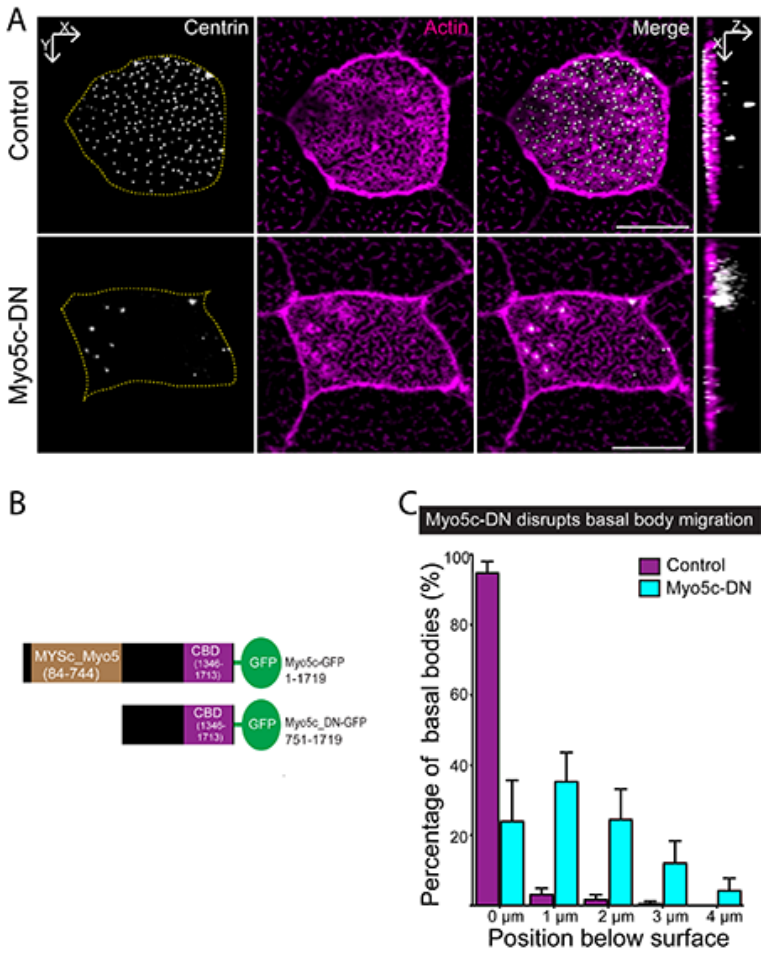

Figure 3.2 Myo5c is required for basal body migration

(A) Overexpression of a dominant negative version of Myo5c (Myo5c-DN-GFP driven by α-tubulin promoter) disrupted basal body migration. In controls（GFP driven by α-tubulin promoter）, most of basal bodies (white) docked within the apical actin network (marked by Phalloidin, magenta, and outlined by a yellow dotted line). Upon overexpression of Myo5c-DN, basal bodies failed to migrate apically and accumulated below the apical surface, see orthogonal views. Scale bar, 10 µm. **(B)** The dominant negative form of Myo5c was generated by truncating the myosin motor domain of Myo5c (84-744 AA) to disrupt its migration ability but left the cargo-binding domain (1346-1713 AA) intact. **(C)** Quantification of basal body positions in controls and upon overexpression of a Myo5c-DN in MCCs. More than 75% of the basal bodies in Myo5c-DN overexpressing cells failed to migrate to the apical surface of MCCs (outlined by a dotted yellow line). The average depth of basal bodies increased from 0.08±0.06 µm in controls to 1.37 ±0.35 µm below the apical domain (reference position, 0 µm) in Myo5-DN, ($P<0.001$; control, n=13 cells; Myo5C-DN, n=14 cells, N>5 embryos. Data represent mean and SD).

3.3 DISCUSSION

Though much evidence suggested that actin was playing a key role in regulating basal body apical migration, its exact function was still unknown until our results showed that actin formed cable structures for basal body transportation. These actin cables were detected only in MCCs and only during basal body migration, suggesting that these cables were specific structures formed for basal body migration. This was further supported by our unpublished data showing that the actin destabilizing protein Gelsolin localized to these cables when they were destroyed. All the evidence implies that these actin cables were tightly regulated specifically for basal body migration. Therefore, it would be of great interest to study how different actin regulators may participate in regulating the dynamics of these actin cables.

Our results showed that Myo5c functioned as the motor for basal body migration along the actin cables. It is still unknown how Myo5c was recruited to basal bodies during its apical migration. The cargo-binding domain is sufficient for its basal body localization, however, how the specificity of cargo binding is determined is still not clear. Some evidence indicates that Myo5c may form a big protein complex with other actin related proteins such as Myo5a and Coronin and others. Myo5a has been reported localizing at basal bodies in primary cilia, and it is possible that these two myosins work together or redundantly. Further, how the polarity of basal body migration is determined is still unknown, it might be determined indirectly by the polarity of actin cables, or directly controlled by the cell polarity machinery such as Par3, which has been showed to control the apical basal polarity of MCC.

In all, our discovery of actin cables and Myo5c as key players in basal body apical migration is just a start to understand the detailed mechanism about this process. Future directions may focus on the mechanism about regulation of actin dynamics and the functional characterization of the predicted protein complex including Myo5c.

Chapter 4: Arhgef18 localized to basal body and was required for basal body docking

4.1 INTRODUCTION

Previously our lab showed that the PCP protein Dishevelled is required for basal body migration, possibly through regulating RhoA signaling activation at basal bodies [4, 8]. RhoA signaling is widely involved in different cellular process, for example RhoA signaling activates many action regulators. Considering our data showing that basal bodies migrated along actin cables and some studies showed that basal bodies might induce nucleation of actin cables, it is highly possible that RhoA signaling is specifically activated at basal bodies for regulation of actin dynamics. However, so far no specific RhoGEF has been identified to be involved in the process.

4.2RESULTS

4.2.1 Arhgef18 localized to basal bodies

By the protein localization screen, we found that ArhGEF18 localized to the basal bodies starting from the early stage of basal body migration to the later stage of basal body docking. The Argef18 showed elongated shapes, and probably marked the striated rootlets.

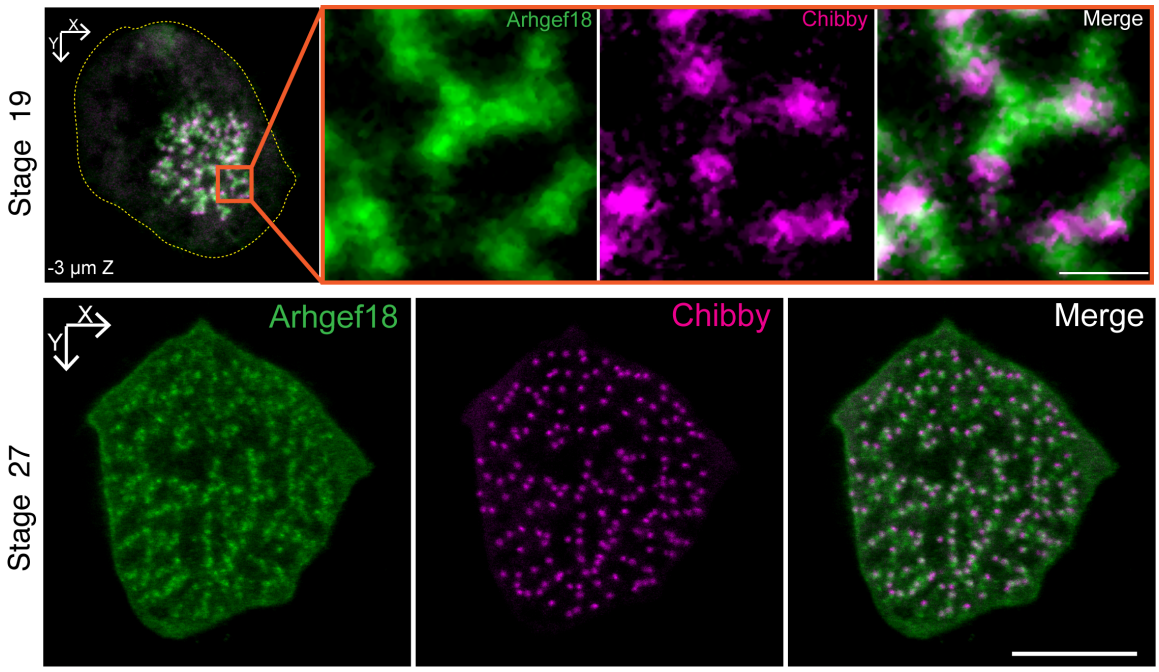

Figure 4.1 Arhgef18 localizes to basal body and cell junctions

Arhgef18 (green) localized to basal bodies (marked by Chibby, magenta) at early stage Stage19**.** Image was taken 3.0 µm below the apical surface of a MCC (outlined by a yellow dotted line). Orange square, zoomed region. Scale bar, 1µm. Arhgef18 localized to both basal bodies and cell junctions at late stage Stage 27.

This localization pattern is of particular interest, because ArhGEF18 has been shown in cell culture experiments localizing to cell junctions and activing RhoA signaling locally at the junctions[9]. We hypothesized that, similar to its function in cell culture, ArhGEF18 might function at the basal body to regulate RhoA signaling activation.

4.2.2 Arhgef18 was required for RhoA signaling activation around basal body

We began to test whether knock down of Arhgef18 would have any effect on RhoA signaling activation. By using the active RhoA sensor rGDB-GFP[8], whose intensity could be measured and taken as quantitative levels of RhoA signaling activation, we confirmed that knocking down Arhgef18 in MCCs significantly reduced the intensities of rGDB-GFP around the basal bodies compared to those in control cells, indicating RhoA signaling activation was reduced upon Arhgef18 knock down.

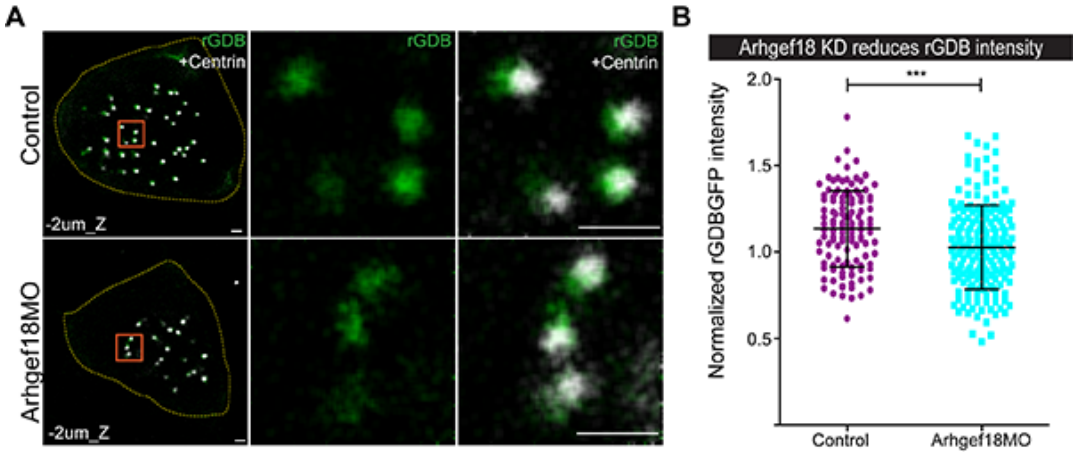

Figure 4.2 Arhgef18 is required for RhoA signaling activation around basal body

The intensity of GFPrGDB was significantly reduced from 1.13 ± 0.22 in control to 1.03±0.24 in arhgef18_Mo cells. (P<0.001; control, n=120 intensities from 6 cells; Arhgef18_MO, n=200 intensities from 10 cells)

4.2.3 Arhgef18 is required for basal body docking

Next, we started to test whether Arhgef18 was required for basal body apical migration. As the results showed, knock down of Arhgef18 severely disrupted basal body docking. Compared with controls in which 95% of the basal bodies docked well at the apical surface, in Arhgef18 knock down groups, over than 70% of basal bodies failed to reach the surface. To further confirm our knockdown data, we used a dominant negative

form of Arhgef18, in which the conserved Y255 was mutated to A to abolish its guanine exchange activity[9]. By specific overexpression of Arhgef18-Y255A in MCCs with an α -tubulin promoter, similar basal body docking defects were determined as Arhgef18 knockdown experiments.

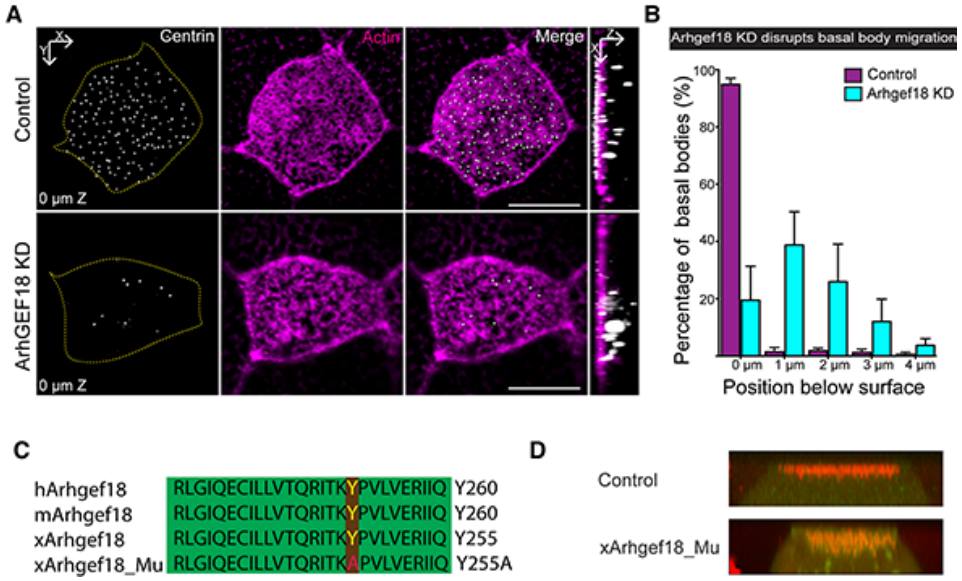

Figure 4.3 Arhgef18 is required for basal body docking

(A) Depletion of Arhgef18 impaired basal body migration. Similarly to expression of a Myo5c-DN, inhibition of Arhgef18 led to basal bodies (marked by Centrin, white) accumulation below the apical surface of a MCC (visualized by actin marker, Phalloidin, magenta, and outlined by a yellow dotted line), see orthogonal sections. Scale bar, 10 µm. **(B)** Quantification of basal bodies position in controls and upon knocknockdownown of Arhgef18 in MCCs. About 95% of the basal bodies in controls docked to the surface of a MCC. In contrast, in Arhgef18 knockdown cells, over 80% of the basal bodies remained below the apical surface (visualized by actin marker, Phalloidin, and outlined by a yellow dotted line). The average depth of basal bodies increased from 0.11±0.05 µm in controls to 1.42 ±0.38 µm below the apical domain (reference position, 0 µm) in Arhgef18 knockdown. ($P<0.001$; control, n=17 cells; Arhgef18 knockdown, n=15 cells, from more than 5 embryos. Data represent mean and SD). **(C)** The dominant negative form of Arhgef118 was generated by mutating conserved Y255 to A. **(D)** Overexpression of Arhgef18_Mu caused severe basal body docking phenotype similar to that of Arhgef18 knock down.

4.3 DISCUSSION

Though RhoA signaling has been shown to be required for basal body dynamic behaviors for over a decade, no more detailed mechanisms have been revealed until our discovery that Arhgef18 localized to basal body and regulated basal body migration through RhoA signaling activation. However, more questions remain to be answered. First, though knocknockdownown of Arhgef18 was sufficient to disrupt basal body docking, we were only able to detect about 15 percent of rGDB-GFP intensity reduction in Arhgef18 knockdown MCCs, so some other RhoA signaling regulators may be functioning at the basal bodies too. Second, how Arhgef18 is recruited to the basal body is still unknown, which might be partially answered by Arhgef18 truncation experiments. Lastly, we still do not know what the relationship is between Arhgef18 and other basal body docking regulators. For example, how does the RhoA signaling control actin cables and Myo5C functions? These different machineries might function in a network to regulate basal body migration together.

Chapter 5: Dennd2b is an actin regulator required for basal body orientation polarity and ciliogenesis

5.1 Introduction

Actin forms tightly regulated network structures at the apical surface of MCC cell cortex[44, 94]. Apical actin networks are composed of two layers of different actin structures, the apical layer forms the lattice structures around the basal bodies, possibly responsible for anchoring the basal body[51], and the subapical actin shows the foci patterns, where the end of striated rootlets are connected to the basal feet of nearby basal bodies[94]. The subapical actin foci are required for basal body spacing and orientation polarity[44]. The formation of the apical cortex actin network requires RhoA activation and some other actin regulators too[50, 95]. However, the molecular mechanism of actin network formation is still largely unknown, especially since very few proteins have been reported to show actin network localization pattern.

5.2 Results

5.2.1 Dennd2b localized to apical cortex actin network and regulated subapical actin foci formation and basal body planar polarities

In the protein localization screen, we found that Dennd2b localized to the MCC cell cortex actin networks, to both the apical and subapical layers. On the apical layer, Dennd2b formed lattice structures around basal bodies similar to that of actin, but with slightly smaller diameters. On the subapical level, Dennd2b colocalized with actin as a foci pattern.

Dennd2b was first identified as a tumor suppressor, and later characterized as an actin regulator localized to leading edge of migrating cells[96]. Patients with Dennd2b mutations showed ciliopathy like syndromes[97, 98]. All of this evidence suggests that Dennd2b may play important functions in MCCs, possibly through regulating actin.

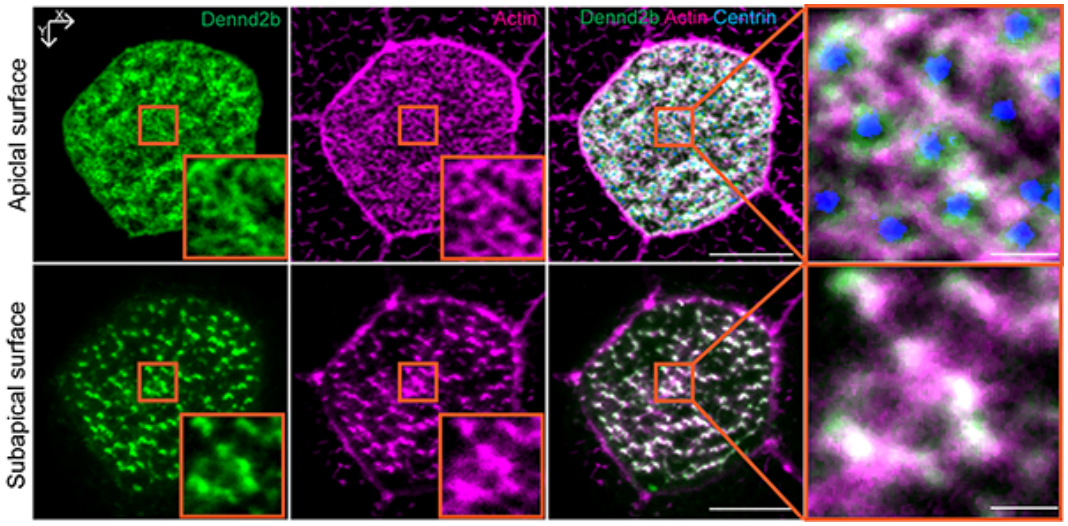

Figure 5.1 Dennd2b localized to cell cortex actin network

GFP-Dennd2b (green) localized to apical and subapical actin network (marked by phalloidin, magenta). Scale bar, 10 μm (in zoomed region, scale bar, 1 μm). Images were taken at stage 32.

First, we started to test whether Dennd2b was required for formation of actin network structures. The Dennd2b morpholino efficiently reduced the transcript level of

Dennd2b. As the results showed, upon knocking down Dennd2b, the apical actin network was slightly affected with less closed lattice structures formed around the basal bodies compared with control cells. The subapical actin foci were greatly reduced from about 60 foci per cell in control samples to about 10 in Dennd2b knockdown cells.

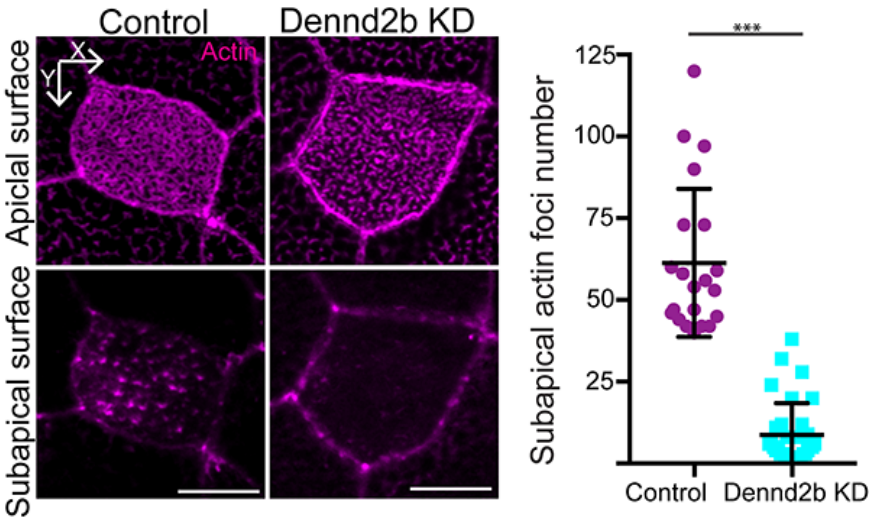

Figure 5.2 Dennd2b is required for formation of subapical actin foci

Dennd2b knockdown reduced the number of subapical actin foci (actin marked by Phalloidin, magenta). Scale bar, 10 µm. The number of subapical actin foci was decreased from 61.3±22.7 in controls to 8.7±9.7 in Dennd2b knockdown ($P<0.001$; Control, n=21 cells; Dennd2b knockdown, n= 33 cells, N>5 embryos). Data represent mean and SD.

The subapical actin network is required for basal body docking and spacing[44, 50], thus it was interesting to determine whether basal body distribution would be affected by Dennd2b knock down. We detected no obvious defects in basal body distribution patterns in Dennd2b knockdown cells, though in some of the cells the basal body tended

to be restricted in the center of MCC apical surfaces, rather than expand to the whole surface.

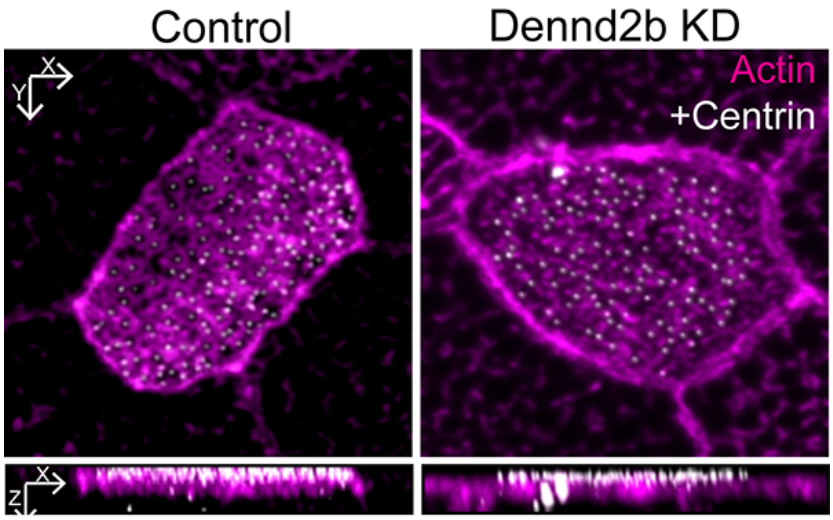

Figure 5.3 Basal body distribution was not disrupted in Dennd2b knocking down MCCs

Dennd2b knockdown did not disrupt basal body docking, actin marked by phalloidin, magenta, side view, lower panel

The subapical actin network is also required for basal body planar polarity[44, 45]. Since the subapical foci were severely disrupted in Dennd2b knock down cells, we were curious to determine whether basal body planar polarities were affected in these Dennd2b knock down cells. By using the strait rootlet marker Clamp, the orientation angles of basal bodies were measured and statistically analyzed. As the results showed,

knocknockdownown of Dennd2b disrupted the planar polarity of basal bodies in MCCs, and these basal bodies showed more random orientations.

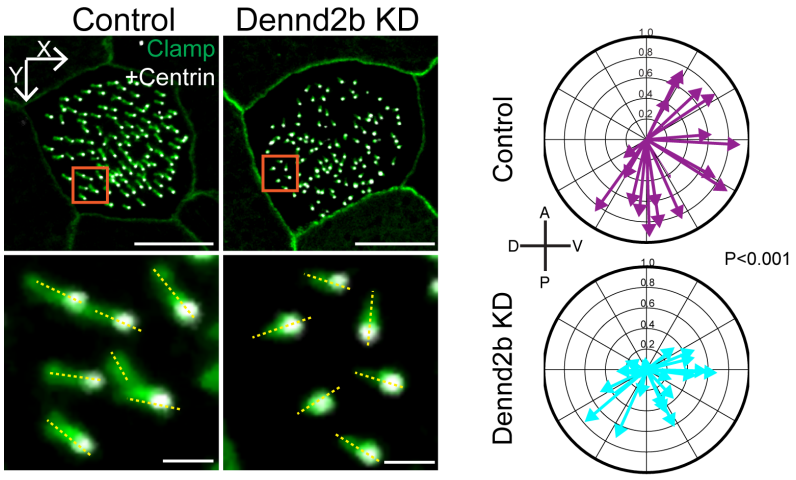

Figure 5.4 Dennd2b is required for basal body orientation polarity

Dennd2b knockdown disrupts basal body orientation. Orientation of basal bodies was determined by measuring angle (yellow dotted line) between a basal body (marked by Centrin4-RFP, white) and corresponding rootlet (marked by Clamp-GFP, green) in respect to the horizontal line. Scale bar, 10 µm (top panel), 1 µm (bottom panel)**.** Quantification of basal bodies orientation. Each arrow represents one cell, where length indicates uniformity of measured angle in that cell (resultant vector). The mean resultant vector value was decreased from 0.71 ± 0.18 in controls to 0.39 ± 0.2 in Dennd2b knockdown. (P<0.001; Control, n=19 cells; Dennd2b knockdown, n= 22 cells, N>5 embryos).

Last, we tried to determine whether Dennd2b was required for other actin regulators' localization to basal bodies. Fak is one of the major actin regulators and is required for basal body docking[51], so we tested whether Fak's localization would be changed by Dennd2b knock down or not. As the results showed, Fak's localization was

not changed upon Dennd2b knockdown[51], as it still localized to basal bodies and striated rootlets.

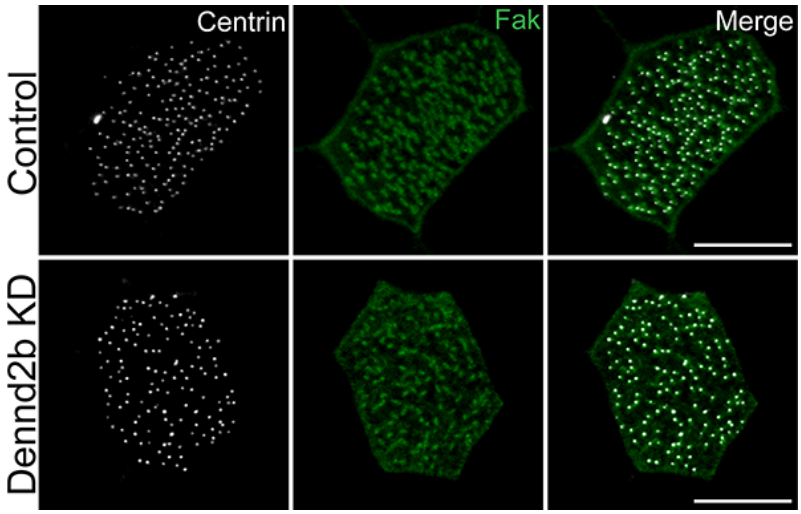

Figure 5.5 Dennd2b is dispensable for Fak localization

Fak (Fak-GFP, green). Scale bar, 10 μm.

5.2.2 Knock down of Dennd2b disrupted ciliogenesis but did not affect IFT20 and Cep164 recruitment

To our surprise, though the basal bodies seemed to be docked in Dennd2b knocknockdownown MCCs, these cells showed severe ciliogenesis defects. The axoneme numbers per MCC were significantly reduced from 67.1 ± 15.4 in control cells to 14.0 ± 8.2 in Dennd2b knocknockdownown cells, and the numbers were slightly rescued to 18.6 ± 8.5 by expression of GFP-Dennd2b with a-tubulin promoter. The ciliogenesis defect phenotype was confirmed by another morpholino knock down and CRISPR knock out experiments.

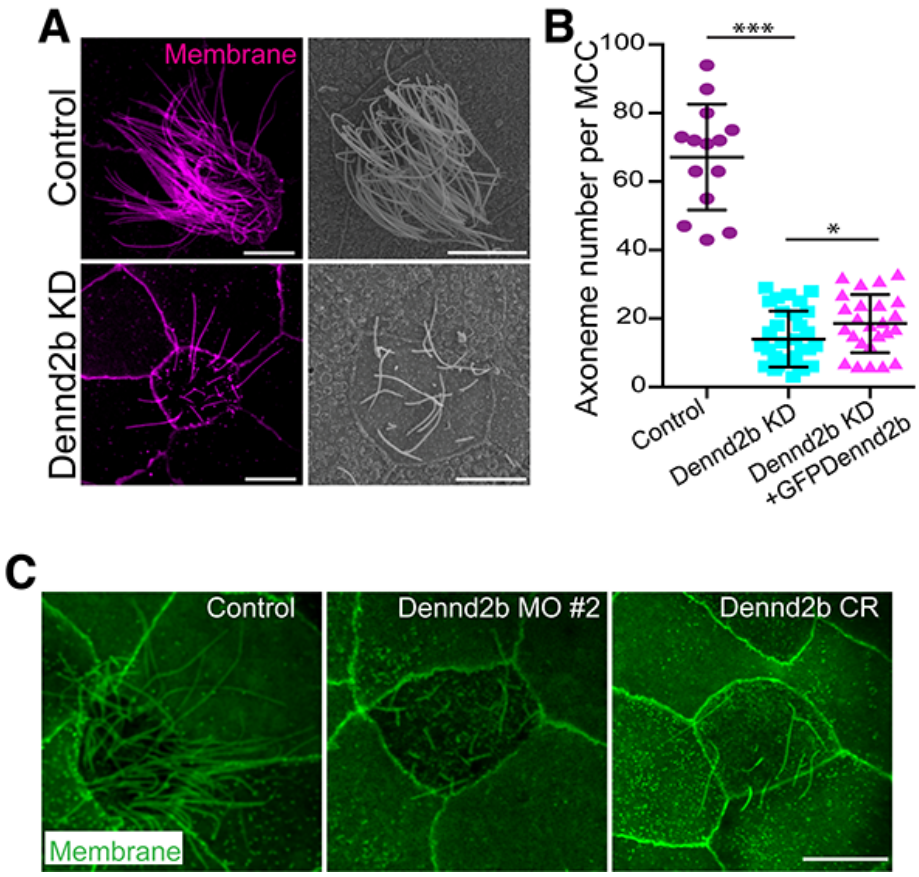

Figure 5.6 Knock down and knock out of Dennd2b induce severe ciliogenesis defects

(A) Perturbation of Dennd2b disrupted ciliogenesis. Left panel, axonemes visualized by CAAX-RFP, magenta. Right panel, SEM of a control MCC and upon Dennd2b knockdown. Scale bar, 10 µm. **(B)** The axoneme number per MCC was significantly reduced from 67.1 ± 15.4 in controls to 14.0 ± 8.2 in Dennd2b knockdown, ($P<0.001$; Control, n=14 cells; Dennd2b knockdown, n= 32 cells, N>5 embryos). Number of axonemes was increased by rescue expression of GFP-Dennd2b with a-tubulin promoter to 18.6 ± 8.5. ($P<0.05$; Dennd2b knockdown with GFP-Dennd2b, n=25 cells, N>5 embryos). Data represent mean and SD. **(C)** Dennd2b MO#2 and Dennd2b CRISPR led to similar axonemogenesis defects as Dennd2b MO#1.

IFT machinery transports substrates for ciliogenesis[99], so we wondered whether IFT recruitment was still functional in Dennd2b knock down cells. Here, we used IFT20 GFP as a marker to check whether IFT recruitment was changed upon Dennd2b knock down.

As the results showed, the intensities of Ift20 around basal bodies were not changed between control and Dennd2b knocknockdownown MCCs, indicating that IFT were still recruited to the basal bodies.

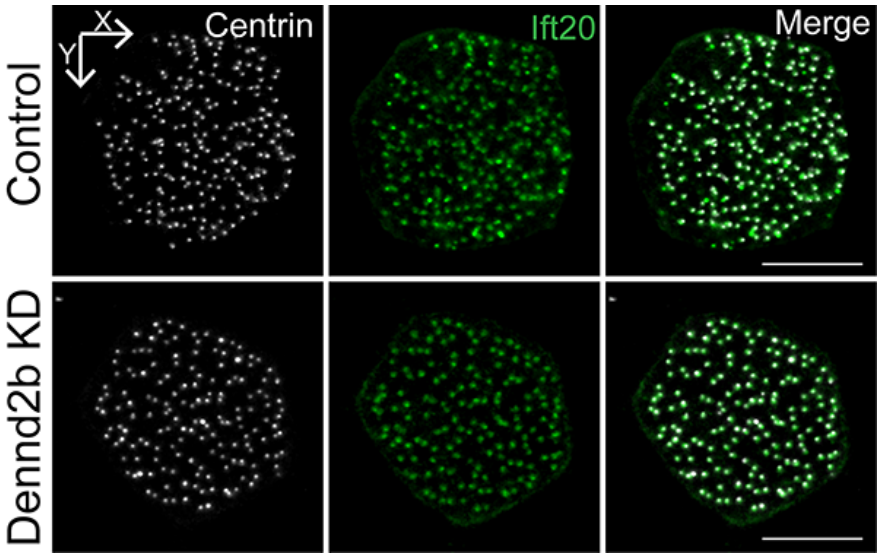

Figure 5.7 IFT recruitment was not disturbed upon Dennd2b knock down

Dennd2b knockdown did not disrupt the recruitment of Ift20 (Ift20-GFP, green). Scale bar, 10 μm.

The transition zone of cilia is required for substrate transportation filtration and recruiting proteins involved in ciliogenesis[100, 101], so we tested whether the transition zone was functional with the transition zone marker Cep164GFP. The results showed that Cep164GFP formed the ring structures both in control and Dennd2b knocknockdownown MCCs.

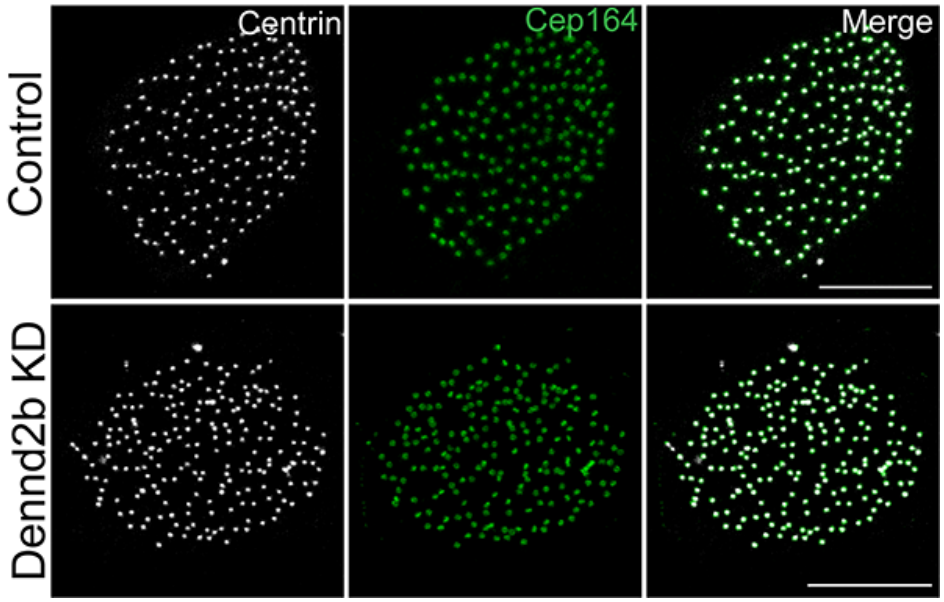

Figure 5.8 Dennd2b knockdown did not disrupt the transition zone structure

The transition zone marker Cep164 labels ring shape transition zone structure in both wild type and Dennd2b morphants. Scale bar, 10 μm.

5.2.3 Dennd2b regulated Ccp110 removal through unknown mechanism

With the results showing that the recruitments of IFTs and transition zone proteins were not disrupted upon Dennd2b knock down, we began to test whether Ccp110 was affected in the morphant cells. Ccp110 is widely used as a molecular marker, which needs to be removed from basal bodies before ciliogenesis[69, 75]. By quantification of Ccp110 levels around basal bodies in both control cells and Dennd2b knock down cells, we found that higher levels of Ccp110 intensity were detected around basal bodies in Dennd2b knockdown cells compared with controls[75], indicating defects of Ccp110 removal in Dennd2b knockdown cells.

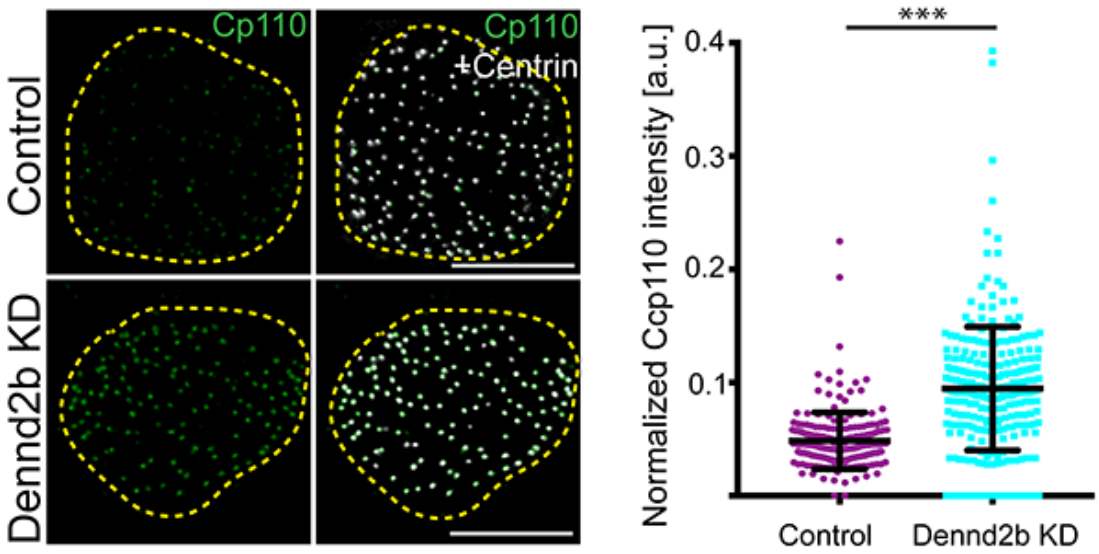

Figure 5.9 Higher Ccp110 intensities were detected in Dennd2b morphants

Dennd2b knockdown increased the level of GFP-Ccp110 (green) at basal bodies (marked by Centrin4-RFP, white). Scale bar, 10 µm. The normalized Ccp110 intensities around basal bodies increased from 0.046 ± 0.045 to 0.093 ± 0.098. ($P<0.001$; Control, n=1430 intensities from 8 cells; Dennd2b knockdown, n= 1413 from 10 cells, N>5 embryos). Data represent mean and SD.

Though the detailed mechanisms about Ccp110 removal are still unknown, some reports showed that Ttbk2, a tubulin kinase, was required for Ccp110 removal[102]. We decided to check whether Ccp110 removal defects detected in Dennd2b knock down MCCs were caused by failure of Ttbk2 recruitment. However, as the results showed, Ttbk2 was recruited to basal bodies and formed ring shape structures in both wildtype and Dennd2b knockdown MCCs, thus the defects of Ccp110 removal was not caused by failure of Ttbk2 recruitment.

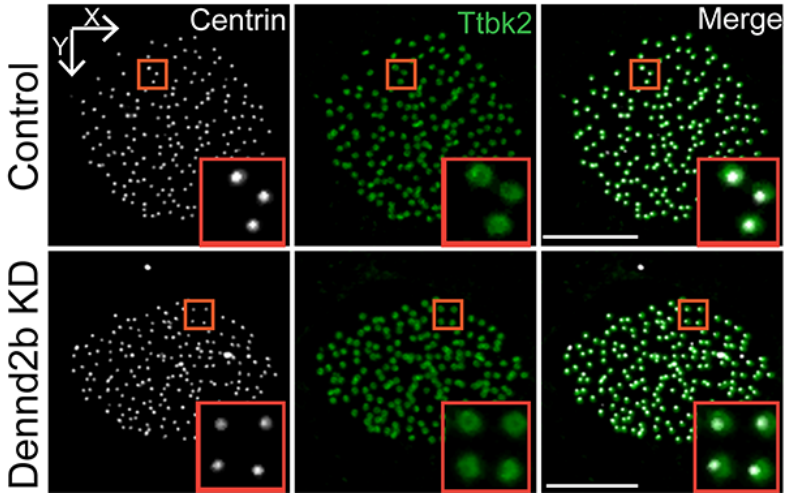

Figure 5.10 Dennd2b is dispensable for Ttbk2 recruitment

Ttbk2 (GFP-Ttbk2, Green) formed a ring shape structure in both wildtype and Dennd2b knockdown MCCs

To further understand how Dennd2b regulated actin dynamic and ciliogenesis, we focused on studying its binding proteins. Drew et al. reported a global map of human protein complexes, one of which showed that Dennd2b might form a protein complex with Myo5a, Afap1, Ablim1 and Cep162[103]. This prediction was of particular interest because of the following reasons. First, most of these proteins were actin related[65, 104, 105], which correlated with Dennd2b's function in actin regulation. Secondly, Myo5a and Cep162 were both required for normal ciliogenesis[65, 105, 106], which correlated with Dennd2b's function in ciliogenesis regulation. All of the evidence suggested that Dennd2b might function through this uncharacterized protein complex including Dennd2b, Myo5a, Afap1, Ablim1 and Cep162, and the phenotypes of Dennd2b knock down MCCs were caused by malfunctions of this Dennd2b containing complex.

So we started with the experiments to test whether Dennd2b was required for the Cep162's localization to the basal bodies in MCCs. The results showed that Cep162 localized to the basal bodies in controls, however, the intensities of Cep162 in Dennd2b knock down cells were significantly reduced, indicating Cep162 failed to localize to the basal bodies without Dennd2b.

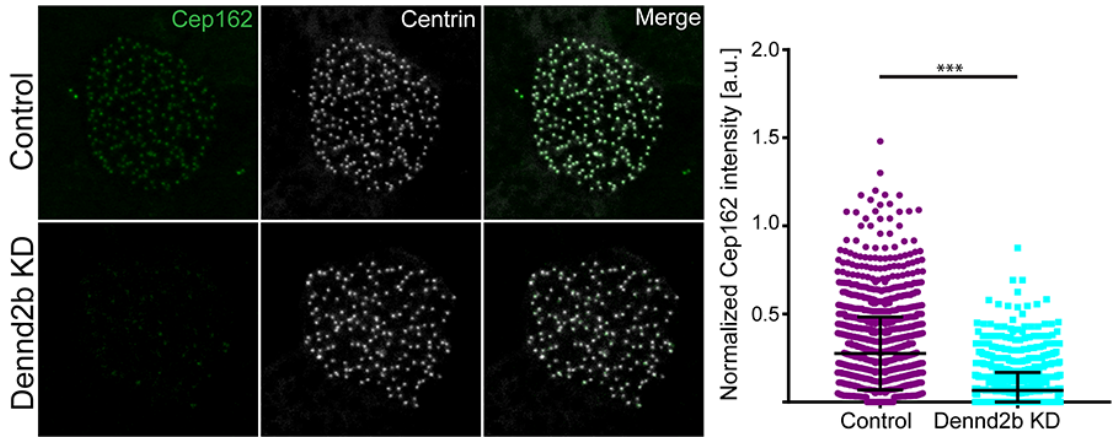

Figure 5.11 The recruitment of Cep162 was abolished upon Dennd2b knock down

Dennd2b knockdown reduced Cep162 intensities around basal bodies. The normalized Cep162 intensities around basal bodies were decreased from 0.28 ± 0.21 to 0.07 ± 0.10. ($P<0.001$; Control, n=1734 intensities from 10 cells; Dennd2b knockdown, n= 1710 from 13 cells, N>5 embryos). Data represent mean and SD.

5.3 Discussion

Though many studies have reported the important functions of MCC apical cortex actin networks, so far very few proteins have been identified to localize to and regulate formation of these actin networks. We found the actin regulator Dennd2b localized to both apical and subapical actin networks, regulated the actin structure integrities, and controlled the ciliary functions such as basal body polarities and ciliogenesis. Dennd2b

may serve as the entry point to understand the detailed molecular mechanisms of the formation and functions of these apical actin structures.

More questions remain to be answered by further studies. First, knocking down of Dennd2b only slightly disrupted the apical actin lattice, indicating other actin regulators might be also involved in this process. Furthermore, very different actin dynamic behaviors have been detected during the formation of these actin network structures, and we still do not know how different actin regulators are involved in this process. Though much evidence has supported the idea that actin dynamics are also tightly related to ciliogenesis, however, the molecular mechanisms connecting these two processes are still unknown. This question might be partially explained by profiling the binding proteins of Dennd2b, which might be the proteins connecting actin dynamics and ciliogenesis regulation. Further experiments are required to confirm whether Dennd2b forms a protein complex with Myo5a, Afap1, Ablim1 and Cep162[103].

Chapter6: Conclusions

Multiciliated cells (MCCs) are essential for the normal functioning of many vertebrate tissues and organs, such as the airway, brain, and reproductive tracts, by generating directional fluid flow[1, 2]. The development of MCCs is a multiple step process that requires cooperation of many different types of cellular machineries[8]. Many studies have focused on the cellular behaviors during the development of MCCs, from cell intercalation to apical emergence, and from ciliogenesis to cilia beating[7, 8, 20, 21]. However, we only know very little about the molecular mechanisms for these cellular behaviors.

Much effort has been made to understand this developmental process systematically on the transcriptome and proteome level[20, 79, 80, 83, 86]. These approaches have identified many candidate genes or proteins that might be involved with ciliary processes, however it is still challenging to systematically study the molecular functions of these possible candidates, especially in the live vertebrate animals. By high content protein localization screen, we identified 199 Rfx2 targets with distinct subcellular localizations to both ciliary structures and non-ciliary structures. Based on this localization data, we selected some of them for further functional studies, because their specific localization patterns indicate that they might participate in ciliary processes. This study serves as a great example to demonstrate the power of high content protein localization screening, which functions as the bridging step between large scale omics data and functional studies on specific proteins.

Basal body apical migration is one of the key cellular behaviors during the development of MCCs. Previous studies have shown that many different proteins, especially actin regulators, were required for this process. Failures of basal body apical migration led to severe ciliogenesis defects[40, 51, 54, 57]. We characterized that specific actin cables were formed, Myo5c functioned as the motor, and Arhgef18 regulated the RhoA signaling activation, for basal body apical migration. These findings further confirmed that actin related machinery was the fundamental molecular mechanism for basal body apical migration. These results also raised more questions to be answered. First, how the actin cables are regulated for basal body migration remains reclusive. It is highly possible different actin regulators are involved. Second, how these proteins are recruited to the basal bodies is still unknown. Myo5c has the cargo binding domain which is able to bring Myo5c to the basal bodies, but it is less clear about how Arhgef18 is recruited. Likewise, as so many different proteins have been reported to be required for basal body trafficking, it is important to study how different proteins cooperate in this process.

The apical actin networks of MCCs have distinct features of structure and function. Many studies have shown that these structures are required for basal body docking, spacing and polarity[44, 45, 107]. By our study, Dennd2b is the first actin regulator to be reported with distinct localization patterns similar to the apical actin network structures in MCCs, and Dennd2b is required for the formation of these structures. The unexpected results showing that Dennd2b was also required for ciliogenesis further supported the long suspected link between actin and ciliogenesis. Further studies are required to

understand the molecular details on how Dennd2b regulates actin dynamics and the molecular networks linking actin and ciliogenesis.

Moreover, besides enhancing our understandings about development of MCCs, our study has also revealed many possible links between Rfx2 targets and human diseases. We identified the subcellular localization of over 40 disease related genes, which may provide important clues to understand the etiology of these diseases. For example, two previous studies have reported patients with Dennd2b mutations that showed typical ciliopathy related syndromes, such as chronic otitis media and recurrent respiratory infections[97, 98]. Our screening data and functional studies on Dennd2b strongly suggest that these patients' syndromes might be due to the MCC defects caused by malfunctions of Dennd2b.

In all, our study demonstrated the power of using a high content protein localization screening approach to facilitate systematical studying on the molecular functions of a large set of protein candidates. These findings not only improved our understanding of different ciliary processes but also revealed many possible and informative links between MCCs and human diseases.

Appendix A EXPERIMENTAL PROCEDURES:

A.1 General scheme for high content protein localization screening in *Xenopus*:

Briefly, using GATEWAY cloning reactions, 260 human open reading frames (ORFs, see below) corresponding to Rfx2 direct target genes [108] were inserted into destination vectors containing N-terminal or C-terminal fluorescent tags along with a MCC specific a-tubulin promoter [109], as indicated in Fig. 1A. All resulting plasmids were then sequenced from both ends. Circular plasmid (~50pg) was then injected into *Xenopus laevis* embryos at the 4-cell stage as described [110]. Plasmids were injected along with membrane-BFP to visualize axonemes, thus ensuring that the localization reported was for MCCs. To speed initial screening, we frequently injected two plasmids encoding different proteins with RFP and GFP tags. Injected embryos were grown and imaged between stages 20 and 31 [111]. Plasmid injection in *Xenopus* is known to result in a wide range of expression levels, based on unequal replication of the plasmids during cell division [110]. Because overexpression can lead to ectopic protein localization, all proteins were examined at a wide range of fluorescent intensities. Proteins for which localization was not consistent across a range of intensities, including very low intensities, were discarded.

A.2 Xenopus handling:

Experiments were performed following the animal ethics guidelines of the University of Texas at Austin, protocol number AUP-2015-00160. *Xenopus laevis* adult females were

induced to ovulate through injection of human chorionic gonadotropin. The following day, eggs were squeezed, fertilized in vitro and dejellied in 3% cysteine (pH 7.9). Fertilized embryos were washed and subsequently reared into 1/3X Marc's Modified Ringer's (MMR) solution. For microinjections, embryos were placed in a solution of 2% Ficoll in 1/3X MMR and injected using glass capillary-pulled needle, forceps, and an Oxford universal micromanipulator.

A.3 HUMAN ORFEOME CLONES:

Gateway entry vectors containing human gene Open Reading Frames (ORFs) were selected from ORFeome library, version 7.1 (*http://horfdb.dfci.harvard.edu/hv7/index.php?page=orfsearch*) [112, 113], distributed by Open Biosystems (GE Dharmacon).

A.4 GATEWAY REACTIONS:

Destination vectors were modified from a destination vector Pcsdest (a gift from Lawson Laboratory) by inserting a MCC-specific α-tubulin promoter (previously described in [108] along with EGFP or mRFP sequences. Fluorescently tagged expression plasmids were made by LR reaction of human ORFeome entry clones and destination vectors containing α-tubulin promoter using Gateway LR Clonase II Enzyme mix (Thermo Fisher Scientific). MCC specific destination vectors were sequenced from both ends for validation.

A.5 *XENOPUS* LAEVIS PLASMIDS:

Myo5C, myo5cDN, Dennd2b, cp110 and ttbk2 were amplified from standard *Xenopus laevis* cDNA prepared by reverse transcription (SuperScriptIII First strand synthesis, Invitrogen) via PCR amplification using the primers listed in Table S4 The PCR products were subcloned into gateway ENTRY clone (pENTR/D-TOPO Cloning Kit, Life Technologies). GFP-FAK is a kind gift from Peter Walentek.

A.6 MORPHOLINO OLIGONUCLEOTIDE AND MRNA INJECTIONS:

Capped RNA was synthesized using mMessage mMachine kits (Life Technologies AM1340). morpholino oligonucleotides (MO) were ordered from GeneTools, LLC. mRNAs and morpholino oligonucleotides at proper concentration were injected into the ventral blastomeres of *Xenopus* embryos at 4 cell stages. morpholino sequences and used concentrations are listed below:

Arhgef18 MO: TCAAAGATTGTCACACTCACCTTCA [14ng]

Dennd2b MO: AGGCATTGATTTACCTGCTTTGGCT [30ng]

Dennd2b MO#2: GGACTGAGACCTGGAAATAAAACAA [10ng]

A.7 XENOPUS ANIMAL CAP QPCR:

Animal cap qPCR assay were used to determine the knock down efficiency of morpholino oligonucleotides, as previously described [108]. Embryos were injected at the

animal side of all 4 cells at four-cell stage with control or morpholino oligonucleotides solutions. Animal caps were collected at stage 9 and used for RNA extraction at different stages. cDNAs were prepared using the Superscript kit (Invitrogen) and qPCR was performed using specific primers listed in Table S4.

A.8 SGRNA SYNTHESIS, CRISPR/CAS9-INDUCED GENOMIC EDITING AND GENOTYPING:
CRISPR/Cas9-mediated genome editing in *Xenopus* was performed as previously described. Briefly, sgRNA was prepared by using the T7 MEGAscript kit (Ambion) and purified by illustra NICK Columns(GE). 500pg Cas9 mRNA and 500pg of sgRNA were injected into the animal pole at the one-cell stage. Genomic DNA was extracted from stage 25 embryos using Wizard® Genomic DNA Purification Kit(Promega). The efficiency of CRISPR/Cas9-mediated genome editing was examined by T7 endonuclease I (T7EI) assay, and DNA fragments were analyzed by 1% agarose gel.

***A.9 XENOPUS* EMBRYO IMAGING:**
Embryos of stages 20-33 were mounted as previously described in [114] and imaged at 23ºC with Zeiss LSM700 confocal microscope using C-Apochromat 40x 1.2 NA water immersion objective or Plan-Apochromat 63x 1.4 NA Oil DIC M27 immersion lens.

A.10 PHALLOIDIN STAINING:

Xenopus embryos were fixed with MEMFA solution at room temperature 2 hours, then washed with PBST, stained with phalloidin solution (15uL phalloidin per 500uL of PBST), incubated for 4 hours at Room Temp and washed with PBST for imaging.

A.11 IN SITU HYBRIDIZATION:

In situ hybridization experiments were performed as described previously[115]. Images were captured with different magnifications on a fluorescent stereomicroscope, Leica MZ16FA.

A.12 BASAL BODY DEPTH QUANTIFICATION:

Basal body numbers were counted manually at each frame of different depth (0,1,2,3,4 μm) below the apical surface of MCCs using Fiji (http://fiji.sc/).

A.13 QUANTIFICATION OF FLUORESCENCE INTENSITIES OF PROTEINS COLOCALIZING WITH BASAL BODIES:

Images were processed and analyzed with Fiji software (http://fiji.sc/). In short, basal bodies were automatically selected by "Find Maxima" function and set the size to "Extra-large" in "Point Tool" function. Intensities of fluorescently tagged proteins of interest and fluorescently tagged basal body markers were measured with the "Measure" function separately. The normalized fluorescence intensity of a candidate protein is a ratio of a

fluorescent intensity of a candidate protein and a fluorescence intensity of a basal body marker.

A.14 Quantification of basal body orientation:

To quantify rootlet orientation, vectors from the tip of the rootlet to the basal body were drawn manually in Fiji (http://fiji.sc/) using maximum intensity projections. The vector length, mean angle, and statistical significance of differences were determined using the CircStat MATLAB Toolbox (Philip Berens, 2009), and Compass plots were generated in MATLAB.

Appendix B The screen lists

Gene Symbol	Synonym	Tagged End	Encoded Protein	Localization	Confidence of localization*	Gene Name	Reported localization in cilia	References
Axoneme	**13**							
ARL4C		C	Full, Isoform 2	Axoneme & Junction	+++	ADP-ribosylation factor-like 4C		
ARMC4		C	Full	Axoneme	++	armadillo repeat containing 4	Axoneme	Hjeij et al., 2013
CCDC19	CFAP45	C	Δ1-85	Axoneme	+++	coiled-coil domain containing 19		
CCDC33		C	Δ230-333	Axoneme	+++	coiled-coil domain containing 33		
CERKL		C	Full	Axoneme & Basolateral membrane	++	ceramide kinase-like protein		
EFHC1		N	Full	Axoneme	+++	EF-hand domain (C-terminal) containing 1	Axoneme	Zhao et al., 2016
EFHC2		N	Full	Axoneme	+++	EF-hand domain (C-terminal) containing 2		
FAM166B		C	Full	Axoneme & Microtubule	+++	family with sequence similarity 166		
IFT140		C	Full	Axoneme	+	intraflagellar transport 140	Axoneme	Perrault et al., 2012
KATNAL2		C	Full, Y6L	Axoneme	+++	katanin p60 subunit A-like 2	Axoneme	Ververis et al., 2016
LRTOMT		C	Full	Axoneme & Fiber in cytosol	+++	leucine rich transmembrane and O-methyltransferase domain containing		
RSPH3		N	Full	Axoneme & Nucleus	++	radial spoke 3 homolog	Axoneme	Jeanson et al., 2015
SPATA13		C	Full, Isoform 2	Axoneme & Cytosol	+++	spermatogenesis associated 13		
Basal Body	**28**							
ABLIM1		N	Full, Isoform P	Basal Body & Foci in cytosol	+++	actin binding LIM protein 1	Actin	Cao et al., 2012
AMOTL2		C	Δ1-103,A3G	Basal Body	+++	angiomotin like 2		
ANKRD45		C	Full	Basal Body	+++	ankyrin repeat domain 45		
BDH1		C	Full,A70S	Basal Body	++	3-hydroxybutyrate dehydrogenase, type 1		

C14ORF45	BBOF1	C	Δ428-529	Basal Body	+++	chromosome 14 open reading frame 45	BB&axoneme	Chien et al., 2013
C1D		C	Full	Basal Body & Everywhere	+	C1D nuclear receptor corepressor		
C6ORF97	CCDC170	C	Full	Basal Body	++	chromosome 6 open reading frame 97		
CCDC65		C	Full	Basal Body & Foci in cytosol	+++	coiled-coil domain-containing protein 65		
EFCAB7		N	Full	Basal Body	++	EF-hand calcium binding domain 7	Basal Body	Pusapati et al., 2014
ELMOD3		N	Full	Basal Body	+++	ELMO/CED-12 domain containing 3		
FAM102B		C	Δ330–360	Basal Body	++	Family with sequence similarity 102, member B		
FAM83A		C	Full	Basal Body-rootlet	++	family with sequence similarity 83, member A		
FBRS		C	Δ1–598,Δ936–970	Basal Body & Golgi	+++	fibrosin		
KIAA1217	SKT	C	Δ1–55	Basal Body	+++	sickle tail protein homolog isoform		
MNS1		N	Full	Basal Body & Foci in cytosol	+++	meiosis-specific nuclear structural 1	sperm flagellum	Vadnais et al., 2014
MTMR11		C	Full, Isoform C	Basal Body	+++	myotubularin related protein 11		
ODF3		C	Full	Basal Body	+	outer dense fiber of sperm tails 3	sperm flagellum	Peterse n et al., 2002
PDE9A		N	Full	Basal Body & Golgi	+++	phosphodiesterase 9A		
PKP2		C	Full	Basal Body & Junction & Axoneme	+++	plakophilin 2		
RASGRP4		C	Full	Basal Body & Axoneme	++	RAS guanyl releasing protein 4		
SESTD1		C	Full	Basal Body & Membrane & Nucleus	+++	SEC14 and spectrin domains 1		
SH3GLB2		C	Full	Basal Body & Cytosol	+	endophilin-B2 isoform b		
TCTN3		N	Full	Basal Body & Foci in cytosol	++	tectonic family member 3		
TRIM37		N	Full	Basal Body & Junction	++	E3 ubiquitin-protein ligase TRIM37	Foci in Cytosol	Balestra et al., 2013
TTC7A		C	Full	Basal Body & Cytosol	++	tetratricopeptide repeat domain 7A		
TTC9C		N	Full	Basal Body & Foci in cytosol	+++	tetratricopeptide repeat domain 9C		
VPS52		N	Full	Basal Body	+++	vacuolar protein sorting 52 homolog		

WDR60		C	Full	Basal Body	+++	WD repeat domain 60	Basal Body	McInerney-Leo et al., 2013
Apical Cortex	**28**							
AFAP1		C	Full	Apical Cortex	+++	actin filament associated protein 1		
B3GNT5		N	Full	Apical Cortex	++	UDP-GlcNAc:betaGal beta-1,3-N-acetylglucosaminyltransferase 5		
C4ORF37	STPG2	N	Full	Apical Cortex & Nucleus	++	sperm-tail PG-rich repeat containing 2		
C7ORF23	TMEM243	C	Full	Apical Cortex & Golgi	+++	chromosome 7 open reading frame 23		
CCDC108		N	Full	Apical Cortex	++	coiled-coil domain containing 108		
CCDC144B		C	Full	Apical Cortex & Junction	+++	coiled-coil domain containing 144B		
CCDC56		C	Full	Apical Cortex & Foci in cytosol	+++	cytochrome c oxidase assembly factor 3		
CRABP2		N	Full	Apical Cortex & Axoneme	+++	cellular retinoic acid binding protein 2		
CYP27A1		C	Full	Apical Cortex	+++	cytochrome P450, family 27, subfamily A, polypeptide 1		
DCTN4		C	Full, Isoform B, A2T	Apical Cortex & Cytosol	++	dynactin 4 (p62)		
FGR		C	Full	Apical Cortex & Basolateral membrane	+++	FGR proto-oncogene, Src family tyrosine kinase		
FMN1		C	Δ498–1196	Apical Cortex	+++	formin 1		
JMY		C	Δ1–354	Apical Cortex	+++	junction mediating and regulatory protein, p53 cofactor		
KCNK1		N	Full	Apical Cortex	+++	potassium channel, subfamily K, member 1		
LPCAT4		C	Full	Apical Cortex	+++	lysophosphatidylcholine acyltransferase 4		
LRP2BP		C	Full	Apical Cortex & Everywhere	+	LRP2-binding protein		
MREG		N	Full	Apical Cortex & Foci in cytosol	+++	melanoregulin		
MYO5C		C	Δ425–1742	Apical Cortex &Basal body	+	myosin VC		

NEXN		C	Δ568–675	Apical Cortex	+++	nexilin (F actin binding protein)		
NHSL2		C	Δ1–287,Δ997–1146	Apical Cortex & Foci in cytosol	++	NHS-like 2		
PALLD		C	Full	Apical Cortex	+++	palladin, cytoskeletal associated protein		
PLS3		N	Full	Apical Cortex	+++	plastin 3		
PSD4		C	Δ417–426	Apical Cortex & Everywhere	++	pleckstrin and Sec7 domain containing 4		
SEMA4D		C	Full	Apical Cortex & Foci in cytosol	+++	sema domain, immunoglobulin domain (Ig), transmembrane domain (TM) and short cytoplasmic domain, (semaphorin) 4D		
SH3GL1		C	Full	Apical Cortex & Junction	+++	SH3-domain GRB2-like 1		
SLC2A13		C	Δ1–19	Apical Cortex & Foci in cytosol	+++	solute carrier family 2 (facilitated glucose transporter), member 13		
DENND2B	Dennd2b	C	Full	Apical Cortex	+++	suppression of tumorigenicity 5		
TUFT1		C	Full	Apical Cortex & Junction	+	tuftelin 1		
Foci in cytosol	**21**							
ALCAM		C	Full	Foci in cytosol	++	activated leukocyte cell adhesion molecule		
C1ORF228		C	Δ308–440	Foci in cytosol_Trafficing foci	+++	chromosome 1 open reading frame 228		
C2ORF77	CCDC173	C	Δ1–6	Foci in cytosol_Trafficing foci	++	chromosome 2 open reading frame 77		
CCDC146		C	Δ1–655	Foci in cytosol_Trafficing foci	+++	coiled-coil domain containing 146	Centrosome of Sperm	Firat-Karalar et al., 2014
CCDC27		C	Full	Foci in cytosol	++	coiled-coil domain containing 27		
CCPG1		C	Δ1–151	Foci in cytosol	+++	cell cycle progression 1		
CELF3		C	Full	Foci in cytosol	+++	CUGBP, Elav-like family member 3		
FAM174A		C	Full	Foci in cytosol_Trafficing foci	+++	family with sequence similarity 174, member A		
FAM92B		C	Full	Foci in cytosol & Basolateral membrane	+++	family with sequence similarity 92	Foci in Cytosol & Basal body	Li et al., 2016

FANK1		C	Full	Foci in cytosol	+	fibronectin type III and ankyrin repeat domains 1		
GORAB		C	Full, Isoform B	Foci in cytosol_Trafficing foci	++	golgin, RAB6-interacting	Golgi	Liu et al., 2016
KIAA0319L		C	Full, Isoform X7	Foci in cytosol	+++	KIAA0319-like		
KRT222		C	Full	Foci in cytosol_Trafficing foci	++	keratin 222 pseudogene		
LSM4		C	Full	Foci in cytosol	+++	SM4 homolog, U6 small nuclear RNA associated		
RAB3A		N	Full	Foci in cytosol_Trafficing foci	+	RAB3A, member RAS oncogene family		
RHOBTB2		C	Full	Foci in cytosol_Trafficing foci	+++	Rho-related BTB domain containing 2		
RIMS2		C	Full, Isoform B	Foci in cytosol_Trafficing foci	+++	regulating synaptic membrane exocytosis 2		
STIP1		C	Full	Foci in cytosol	+++	stress-induced-phosphoprotein 1 (Hsp70/Hsp90-organizing protein)		
TBC1D9		C	Full	Foci in cytosol_Trafficing foci	+++	TBC1 domain family member 9		
TBCCD1		C	Full	Foci in cytosol	+++	TBCC domain containing 1	Foci in Cytosol & Basal body	Gonçalves et al., 2010
TMEM185A		C	Full	Foci in cytosol_Trafficing foci	+++	transmembrane protein 185A		
Golgi	**13**							
ARFGAP3		C	Full	Golgi	+++	ADP-ribosylation factor GTPase activating protein 3		
C11ORF70		C	Δ1–38	Golgi	+	chromosome 11 open reading frame 70		
COL4A3BP		C	Full, Isoform 2, K594Q	Golgi	++	collagen, type IV, alpha 3 (Goodpasture antigen) binding protein		
CXADR		C	Full	Golgi	++	coxsackie virus and adenovirus receptor		
FURIN		C	Full	Golgi	+++	furin (paired basic amino acid cleaving enzyme)		
GALNT4		N	Full	Golgi & ER	+++	polypeptide N-acetylgalactosaminyltransferase 4		
GALNT5		C	Δ486–956	Golgi	+++	polypeptide N-acetylgalactosaminyltransferase 5		

GMPR2		N	Full	Golgi & Trafficing foci	+++	guanosine monophosphate reductase 2		
GOLM1		C	Full	Golgi	+++	golgi membrane protein 1		
MYOF		C	Δ1232–1729	Golgi	+++	myoferlin		
NIPAL1		C	Full	Golgi & Trafficing foci	+++	NIPA-like domain containing 1		
TMED7		C	Full	Golgi	++	transmembrane emp24 protein transport domain containing 7		
TMEM110		C	Full	Golgi & Trafficing foci	+++	transmembrane protein 110		
Mitochondria	**5**							
C1ORF201	MAPO2	C	Full, Isoform 3	Mitochondria & Axoneme	++	chromosome 1 open reading frame 201		
CPSF4		C	Full	Mitochondria	++	cleavage and polyadenylation specific factor 4, 30knockdowna		
DAP3		C	Full	Mitochondria	+++	death associated protein 3		
PLEKHG7		C	Full	Mitochondria	++	pleckstrin homology domain containing, family G (with RhoGef domain) member 7		
TTC39B		C	Δ1–456	Mitochondria	+	tetratricopeptide repeat domain 39B		
Cytosol	**36**							
AIFM3		N	Full	Cytosol	++	apoptosis-inducing factor, mitochondrion-associated, 3		
ANXA2		C	Full,Isoform 2	Cytosol	+++	annexin A2		
ARHGEF10L		C	Full	Cytosol	+++	Rho guanine nucleotide exchange factor (GEF) 10-like		
ARPC1A		C	Full	Cytosol	+++	actin related protein 2/3 complex, subunit 1A, 41knockdowna		
BIN3		C	Full,F6L	Cytosol	+++	bridging integrator 3		
C10ORF88		C	Full	Cytosol	+++	chromosome 10 open reading frame 88		
C20ORF26	CFAP61	C	Full	Cytosol	+	chromosome 20 open reading frame 26		
C21ORF59	KURLY	N	Full	Cytosol	+++	chromosome 21 open reading frame 59	Cytosol	Jaffe et al., 2016

C7ORF46	FAM221A	C	Full,T34I	Cytosol	+	chromosome 7 open reading frame 46		
CARS		C	Full, Isoform B	Cytosol	+++	cysteinyl-tRNA synthetase		
CCDC104	CFAP36,BARTL1	C	Full	Cytosol	+++	coiled-coil domain containing 104	Cytosol & Axoneme	Lokaj et al., 2015
CCDC6		C	Full	Cytosol	+++	coiled-coil domain containing 58		
CCT2		C	Full	Cytosol	+++	chaperonin containing TCP1, subunit 2 (beta)		
CDC25C		C	Full	Cytosol	+++	cell division cycle 25 homolog C (S. pombe)		
DIS3L2		C	Δ1–7Δ581–885	Cytosol	+	DIS3 mitotic control homolog (S. cerevisiae)-like 2		
EFCAB2		C	Full	Cytosol	+++	EF-hand calcium binding domain 2		
ELMO1		C	Full	Cytosol	+++	engulfment and cell motility 1	Basal Body & Axoneme	Epting et al., 2015
FAM195B	MCRIP1	C	Full	Cytosol	+	hypothetical protein LOC348262		
FLNA		C	Δ1–1754	Cytosol	+++	filamin A, alpha		
KCNRG		C	Full	Cytosol	+++	potassium channel regulator		
LEPREL1		N	Full	Cytosol	+++	leprecan-like 1		
LEPREL2	P3H3	N	Δ1–185	Cytosol	++	leprecan-like 2		
NAA30		C	Full	Cytosol	+++	N-acetyltransferase 12 (GCN5-related, putative)		
NPEPPS		C	Full	Cytosol	+++	aminopeptidase puromycin sensitive		
NUMBL		C	Full,N2K	Cytosol	+++	numb homolog (Drosophila)-like		
PFKP		C	Full	Cytosol	+++	phosphofructokinase, platelet		
PFN2		C	Full	Cytosol	++	profilin 2		
PRKCB		N	Full	Cytosol	++	protein kinase C, beta		
RABL2B		C	Full	Cytosol	++	RAB, member of RAS oncogene family-like 2B		
REC8		C	Full	Cytosol	++	REC8 homolog (yeast)		
TFAP2A		C	Full	Cytosol	+++	transcription factor AP-2 alpha		
TSGA10		N	Full	Cytosol	+++	ER-Golgi vesicle-tethering protein p115	Cytosol	Ivliev et al., 2012

UQCRQ		C	Full	Cytosol	+++	low molecular mass ubiquinone-binding protein (9.5knockdown)		
WDR88		C	Δ422-428,A2V	Cytosol	+++	WD repeat domain 88		
WDR92		C	Full, Isoform B	Cytosol	+	WD repeat domain 92		
ZFAND5		C	Full	Cytosol	+++	zinc finger, AN1-type domain 5		
ER	**21**							
ATG9B		C	Δ1–569	ER & Mitochondria	+	ATG9 autophagy related 9 homolog B (S. cerevisiae)		
AVPR2		C	Full	ER	+++	AVPR2 arginine vasopressin receptor 2		
C5ORF62	SMIM3	C	Full	ER	+++	SMIM3		
CCDC155		C	Full	ER	+++	coiled-coil domain containing 155		
CCDC167		C	Full	ER	+++	coiled-coil domain containing 167		
CYB5B		C	Δ1-4,L52P	ER	+++	cytochrome b5 type B (outer mitochondrial membrane)		
DHRS3		C	Full	ER	+	dehydrogenase/reductase (SDR family) member 3		
DNAJB14		C	Full	ER	+++	DnaJ (Hsp40) homolog, subfamily B, member 14		
KIF1C		C	Full	ER	++	kinesin-like protein KIF1C		
NOTCH2		C	Full	ER	+++	neurogenic locus notch homolog protein 2		
PDIA6		C	Full, Isoform D	ER	+++	thioredoxin domain containing 7 (protein disulfide isomerase)		
PLOD3		C	Full	ER	++	procollagen-lysine, 2-oxoglutarate 5-dioxygenase 3		
SLC22A5		N	Full	ER	+++	solute carrier family 22 member 5		
SLC4A1		C	Full	ER	+++	solute carrier family 4 (anion exchanger), member 1	Axoneme	Hengl et al., 2010
SPARC		C	Full	ER & Apical cortex	+++	secreted protein, acidic, cysteine-rich (osteonectin)	Axoneme	Huynh et al., 2000
THEM4		C	Full	ER	+	thioesterase superfamily member 4		
TMEM18		C	Δ1–19	ER	+++	transmembrane protein 18		
TMEM194A	NEMP1	C	Full, Isoform B	ER	+++	transmembrane protein 194A		

TMEM203		C	Full	ER	+++	transmembrane protein 203		
TMEM38B		C	Full	ER	+++	transmembrane protein 38B		
VASN		N	Full	ER	+++	vasorin		
Nucleus	**22**							
ADARB1		C	Full	Nucleus	+++	adenosine deaminase, RNA-specific, B1		
BCL7A		C	Full	Nucleus	+++	B-cell CLL/lymphoma 7A		
BCL7B		C	Full,S200A	Nucleus	+++	B-cell CLL/lymphoma 7B		
C14ORF79		C	Δ1–242	Nucleus	+++	chromosome 14 open reading frame 79		
CCDC12		C	Full	Nucleus	+++	coiled-coil domain containing 12		
CCDC76		C	Full	Nucleus	++	tRNA methyltransferase 13 homolog		
CCNA1		C	Full	Nucleus	+++	cyclin A1		
CDC25B		C	Full	Nucleus	++	cell division cycle 25B		
CDKN1B		C	Full	Nucleus	+++	cyclin-dependent kinase inhibitor 1B (p27, Kip1)		
DLX3		C	Full	Nucleus	++	distal-less homeobox 3		
DLX4		C	Full	Nucleus	+++	distal-less homeobox 4		
ETV1		C	Full	Nucleus	+++	ets variant 1		
FAM161A		C	Full, isoform X1	Nucleus & Microtubule	+++	family with sequence similarity 161, member A	Microtubule	Zach et al., 2012
FAM76B		C	Δ231–339	Nucleus	+++	family with sequence similarity 76, member B		
KIF22		N	Full	Nucleus	+	kinesin family member 22		
LMNA		C	Full	Nucleus	+++	lamin A/C		
PIF1		C	Full	Nucleus	+++	PIF1 5'-to-3' DNA helicase		
PTPN6		N	Full	Nucleus	+++	protein tyrosine phosphatase, non-receptor type 6		
RANBP3L		C	Full	Nucleus	+++	RAN binding protein 3-like		
TIAL1		C	Δ1–124	Nucleus & Foci in cytosol	+++	TIA1 cytotoxic granule-associated RNA binding protein-like 1		
TPRN		C	Δ1–306	Nucleus	+++	taperin		

WDR5		C	Full	Nucleus	+++	WD repeat domain 5		
Others	**12**							
C3ORF38		C	Full	others_Membrane	++	chromosome 3 open reading frame 38		
C9ORF89	CARD19	C	Full	others_fibers	+++	chromosome 9 open reading frame 89		
CDC14A		C	Full	others_short segment on apical Cortex	+++	cell division cycle 14A		
FAM125B	MVB12B	C	Full	others_Basolateral membrane	+++	family with sequence similarity 125, member B		
FAM190A		C	Full, Isofrom 2	others_Membrane	++	KIAA1680 protein		
MAP2		C	Full, Isoform 5	Others_Microtubule & Axoneme	+++	microtubule-associated protein 2		
POF1B		N	Full	others_Junction	+++	premature ovarian failure, 1B		
RASEF		C	Full	others_Aggregates in the center	++	RAS and EF-hand domain containing		
SPECC1L		C	Full	others_fibers	++	sperm antigen with calponin homology and coiled-coil domains 1-like		
SPRED1		C	Full	others_Basolateral membrane & big foci	+++	sprouty-related, EVH1 domain containing 1		
SYT5		C	Full	others_Membrane	+	synaptotagmin V		
TUSC5		C	Full	others_Basolateral membrane & Golgi	+++	tumor suppressor candidate 5		
Everywhere	**36**							
ACY3		C	Full	Everywhere	+++	aspartoacylase (aminocyclase) 3		
ADORA2A		C	Full	Everywhere	+	adenosine A2a receptor		
ANXA9		C	$\Delta 1-7$	Everywhere	+	annexin A9		
C11ORF49		C	Full	Everywhere	+++	chromosome 11 open reading frame 49		
C11ORF65		C	Full	Everywhere	+++	chromosome 11 open reading frame 65		
C12ORF45		C	Full	Everywhere	+++	chromosome 12 open reading frame 45		
C19ORF40	FAAP24	C	Full,K3N	Everywhere	+++	chromosome 19 open reading frame 40		

C21ORF33		C	Full	Everywhere	+++	chromosome 21 open reading frame 33		
C2ORF62	CATIP	C	Full, isoform 2	Everywhere	+++	chromosome 2 open reading frame 62	Everywhere	Bontems et al., 2014
C2ORF67	KANSL1	C	Full	Everywhere	+++	chromosome 2 open reading frame 67		
C2ORF73		C	Full, Isoform X3, P133L	Everywhere	+++	chromosome 2 open reading frame 73		
C7ORF63	CFAP69	C	Full	Everywhere	+	chromosome 7 open reading frame 63		
C9ORF116		C	Full, isoform 2	Everywhere	+++	chromosome 9 open reading frame 116		
CCDC58		C	Full	Everywhere	+++	coiled-coil domain containing 58		
CHCHD4		C	Full	Everywhere	+++	mitochondrial intermembrane space import and assembly protein 40coiled-coil-helix-coiled-coil-helix domain containing 4		
EFHD1		N	Full	Everywhere	++	EF-hand domain family, member D1		
FAIM		C	Full	Everywhere	+++	Fas apoptotic inhibitory molecule		
FAM102A		C	Full	Everywhere	+++	family with sequence similarity 102, member A		
FAM173A		C	Full	Everywhere	+++	family with sequence similarity 173		
GLO1		C	Full, Y19C	Everywhere	+++	glyoxalase I		
HDAC10		C	Full	Everywhere	+	histone deacetylase 10		
KIAA0513		C	Full, Isoform C	Everywhere	+++	KIAA0513		
MED10		C	Full	Everywhere	+++	mediator complex subunit 10		
MID1IP1		C	Full	Everywhere	+++	MID1 interacting protein 1 (gastrulation specific G12 homolog (zebrafish))		
NCAPG		C	Full,R6M	Everywhere	+	non-SMC condensin I complex, subunit G		
PARD6B		C	Full	Everywhere	++	par-6 partitioning defective 6 homolog beta (C. elegans)		
PELO		C	Full	Everywhere	+++	pelota homolog (Drosophila)		
RAB28		N	Full	Everywhere	+++	RAB28, member RAS oncogene family	Axoneme	Jensen et al., 2016
RAP2C		C	Full	Everywhere	+++	RAP2C, member of RAS oncogene family		

SPATA4		C	Full	Everywhere	+++	spermatogenesis associated 4		
SPEG		C	Full, Isoform 4	Everywhere	+++	SPEG complex locus		
TNFAIP8 L2		C	Full	Everywhere	+++	tumor necrosis factor alpha-induced protein 8-like protein 2		
TTC18	CFAP70	C	Full	Everywhere	+	tetratricopeptide repeat domain 18		
TXNDC5		C	Δ1–88	Everywhere	+++	thioredoxin domain containing 5 (endoplasmic reticulum)		
USP42		C	Full	Everywhere	+	ubiquitin carboxyl-terminal hydrolase 42		
WDR49		C	Full	Everywhere	+++	WD repeat domain 49		
No Signal	**25**							
ACAP3		C	Full	NS		ArfGAP with coiled-coil, ankyrin repeat and PH domains 3		
ARRDC3		C	Full	NS		arrestin domain containing 3		
BGN		N	Full	NS		biglycan		
C12ORF52		C	Full	NS		chromosome 12 open reading frame 52		
C8ORF34		N	Full	NS		chromosome 8 open reading frame 34		
CAPN13		C	Full	NS		calpain 13		
CASC1		C	Full	NS		cancer susceptibility candidate 1		
CCDC60		N	Full	NS		coiled-coil domain containing60		
CCDC90A		C	Full	NS		mitochondrial calcium uniporter regulator 1		
CYCS		C	Full	NS		cytochrome c, somatic		
DDIT4		C	Full	NS		DNA-damage-inducible transcript 4		
DNAJB9		C	Full	NS		DnaJ (Hsp40) homolog, subfamily B, member 9		
DNAJC27		C	Full	NS		DnaJ (Hsp40) homolog, subfamily C, member 27		
HADHA		C	Full	NS		hydroxyacyl-Coenzyme A dehydrogenase/3-ketoacyl-Coenzyme A thiolase/enoyl-Coenzyme A hydratase (trifunctional protein),		

						alpha subunit		
HSPH1		C	Full	NS		heat shock 105knockdowna/110 knockdowna protein 1		
ITGA5		C	Full	NS		integrin, alpha 5 (fibronectin receptor, alpha polypeptide)		
JUN		N	Full	NS		jun proto-oncogene		
KIAA1191		C	Full	NS		KIAA1191		
LMCD1		N	Full	NS		LIM and cysteine-rich domains 1		
PLK3		C	Full	NS		polo-like kinase 3 (Drosophila)		
S1PR2		C	Full	NS		sphingosine-1-phosphate receptor 2		
SLC25A29		C	Full	NS		solute carrier family 25 member 29		
SPG7		C	Δ428−795	NS		spastic paraplegia 7		
WDR63		C	Full,V890E	NS		WD repeat domain 63		
WDR93		C	Full	NS		WD repeat domain 93		
Totals:								
Mitochondria	**5**							
Others	**12**							
Axoneme	**13**							
Golgi	**13**							
Foci in cytosol	**21**							
ER	**21**							
Nucleus	**22**							
No Signal	**25**							
Basal Body	**28**							
Apical Cortex	**28**							

Cytosol	**36**							
Everywhere	**36**							
Total	**260**							
References								

Balestra, F. R., Strnad, P., Flückiger, I. and Gönczy, P. (2013). Discovering regulators of centriole biogenesis through siRNA-based functional genomics in human cells. Developmental cell 25, 555-571.

Bontems, F., Fish, R. J., Borlat, I., Lembo, F., Chocu, S., Chalmel, F., Borg, J.-P., Pineau, C., Neerman-Arbez, M., Bairoch, A., et al. (2014). C2orf62 and TTC17 Are Involved in Actin Organization and Ciliogenesis in Zebrafish and Human. PLoS ONE 9, e86476.

Cao, J., Shen, Y., Zhu, L., Xu, Y., Zhou, Y., Wu, Z., Li, Y., Yan, X. and Zhu, X. (2012). miR-129-3p controls cilia assembly by regulating CP110 and actin dynamics. Nature cell biology 14, 697-706.

Chien, Y.-H., Werner, M. E., Stubbs, J., Joens, M. S., Li, J., Chien, S., Fitzpatrick, J. A. J., Mitchell, B. J. and Kintner, C. (2013). Bbof1 is required to maintain cilia orientation. Development 140, 3468-3477.

Epting, D., Slanchev, K., Boehlke, C., Hoff, S., Loges, N. T., Yasunaga, T., Indorf, L., Nestel, S., Lienkamp, S. S. and Omran, H. (2015). The Rac1 regulator ELMO controls basal body migration and docking in multiciliated cells through interaction with Ezrin. Development 142, 174-184.

Firat-Karalar, E. N., Sante, J., Elliott, S. and Stearns, T. (2014). Proteomic analysis of mammalian sperm cells identifies new components of the centrosome. J Cell Sci 127, 4128-4133.

Gonçalves, J., Nolasco, S., Nascimento, R., Fanarraga, M. L., Zabala, J. C. and Soares, H. (2010). TBCCD1, a new centrosomal protein, is required for centrosome and Golgi apparatus positioning. EMBO reports 11, 194-200.

Hengl, T., Kaneko, H., Dauner, K., Vocke, K., Frings, S. and Möhrlen, F. (2010). Molecular components of signal amplification in olfactory sensory cilia. Proceedings of the National Academy of Sciences 107, 6052-6057.

Hjeij, R., Lindstrand, A., Francis, R., Zariwala, M. A., Liu, X., Li, Y., Damerla, R., Dougherty, G. W., Abouhamed, M. and Olbrich, H. (2013). ARMC4 mutations cause primary ciliary dyskinesia with randomization of left/right body asymmetry. The American Journal of Human Genetics 93, 357-367.

Huynh, M. H., Hong, H., Delovitch, S., Desser, S. and Ringuette, M. (2000). Association of SPARC (osteonectin, BM-40) with extracellular and intracellular components of the ciliated surface ectoderm of *Xenopus* embryos. Cell motility and the cytoskeleton 47, 154-162.

Ivliev, A. E., AC't Hoen, P., van Roon-Mom, W. M., Peters, D. J. and Sergeeva, M. G. (2012). Exploring the transcriptome of ciliated cells using in silico dissection of human tissues. PLoS One 7, e35618.

Jaffe, K. M., Grimes, D. T., Schottenfeld-Roames, J., Werner, M. E., Ku, T.-S. J., Kim, S. K., Pelliccia, J. L., Morante, N. F., Mitchell, B. J. and Burdine, R. D. (2016). c21orf59/kurly controls both cilia motility and polarization. Cell reports 14, 1841-1849.

Jeanson, L., Copin, B., Papon, J.-F., Dastot-Le Moal, F., Duquesnoy, P., Montantin, G., Cadranel, J., Corvol, H., Coste, A. and Désir, J. (2015). RSPH3 mutations cause primary ciliary dyskinesia with central-complex defects and a near absence of radial spokes. The American Journal of Human Genetics 97, 153-162.

Jensen, V. L., Carter, S., Sanders, A. A., Li, C., Kennedy, J., Timbers, T. A., Cai, J., Scheidel, N., Kennedy, B. N. and Morin, R. D. (2016). Whole-Organism Developmental Expression Profiling Identifies RAB-28 as a Novel Ciliary GTPase Associated with the BBSome and Intraflagellar Transport. PLoS Genetics 12, e1006469.

Li, F.-Q., Chen, X., Fisher, C., Siller, S. S., Zelikman, K., Kuriyama, R. and Takemaru, K.-I. (2016). BAR Domain-Containing FAM92 Proteins Interact with Chibby1 To Facilitate Ciliogenesis. Molecular and Cellular Biology 36, 2668-2680.

Liu, Y., Snedecor, E. R., Choi, Y. J., Yang, N., Zhang, X., Xu, Y., Han, Y., Jones, E. C., Shroyer, K. R. and Clark, R. A. (2016). Gorab Is Required for Dermal Condensate Cells to Respond to Hedgehog Signals during Hair Follicle Morphogenesis. Journal of Investigative Dermatology 136, 378-386.

Lokaj, M., Kösling, S. K., Koerner, C., Lange, S. M., Van Beersum, S. E., Van Reeuwijk, J., Roepman, R., Horn, N., Ueffing, M. and Boldt, K. (2015). The interaction of CCDC104/BARTL1 with Arl3 and implications for ciliary function. Structure 23, 2122-2132.

McInerney-Leo, A. M., Schmidts, M., Cortés, C. R., Leo, P. J., Gener, B., Courtney, A. D., Gardiner, B., Harris, J. A., Lu, Y. and Marshall, M. (2013). Short-rib polydactyly and Jeune syndromes are caused by mutations in WDR60. The American Journal of Human Genetics 93, 515-523.

Perrault, I., Saunier, S., Hanein, S., Filhol, E., Bizet, A. A., Collins, F., Salih, M. A., Gerber, S., Delphin, N. and Bigot, K. (2012). Mainzer-Saldino syndrome is a ciliopathy caused by IFT140 mutations. The American Journal of Human Genetics 90, 864-870.

Petersen, C., Aumüller, G., Bahrami, M. and Hoyer-Fender, S. (2002). Molecular cloning of Odf3 encoding a novel coiled-coil protein of sperm tail outer dense fibers*. Molecular reproduction and development 61, 102-112.

Pusapati, G. V., Hughes, C. E., Dorn, K. V., Zhang, D., Sugianto, P., Aravind, L. and Rohatgi, R. (2014). EFCAB7 and IQCE regulate hedgehog signaling by tethering the EVC-EVC2 complex to the base of primary cilia. Developmental cell 28, 483-496.

Vadnais, M. L., Lin, A. M. and Gerton, G. L. (2014). Mitochondrial fusion protein MFN2 interacts with the mitostatin-related protein

MNS1 required for mouse sperm flagellar structure and function. Cilia 3, 5.
Ververis, A., Christodoulou, A., Christoforou, M., Kamilari, C., Lederer, C. W. and Santama, N. (2016). A novel family of katanin-like 2 protein isoforms (KATNAL2), interacting with nucleotide-binding proteins Nubp1 and Nubp2, are key regulators of different MT-based processes in mammalian cells. Cellular and Molecular Life Sciences 73, 163-184.
Zach, F., Grassmann, F., Langmann, T., Sorusch, N., Wolfrum, U. and Stöhr, H. (2012). The retinitis pigmentosa 28 protein FAM161A is a novel ciliary protein involved in intermolecular protein interaction and microtubule association. Human molecular genetics 21, 4573-4586.
Zhao, Y., Shi, J., Winey, M. and Klymkowsky, M. W. (2016). Identifying domains of EFHC1 involved in ciliary localization, ciliogenesis, and the regulation of Wnt signaling. Developmental biology 411, 257-265.

Table B1 The list shows the information about the genes included in the protein localization screen

Table B2			
Gene Symbol	Localization	Confidence of localization*	OMIM
ARMC4	Axoneme	++	Ciliary dyskinesia, primary, 23, 615451 (3), Autosomal recessive
AVPR2	ER	+++	Diabetes insipidus, nephrogenic, 304800 (3), X-linked recessive; Nephrogenic syndrome of inappropriate antidiuresis, 300539 (3), X-linked recessive
BCL7A	Nucleus	+++	B-cell non-Hodgkin lymphoma, high-grade (3)
C21ORF59	Cytosol	+++	Ciliary dyskinesia, primary, 26, 615500 (3), Autosomal recessive
CCDC65	Mitochondria	+++	Ciliary dyskinesia, primary, 27, 615504 (3), Autosomal recessive
CDC14A	others_short segment on Apical Cortex	+++	Deafness, autosomal recessive 105, 616958 (3), Autosomal recessive
CDKN1B	Nucleus	+++	Multiple endocrine neoplasia, type IV, 610755 (3), Autosomal dominant
CERKL	Axoneme & Basolateral Membrane	++	Retinitis pigmentosa 26, 608380 (3)
COL4A3BP	Golgi	++	Mental retardation, autosomal dominant 34, 616351 (3), Autosomal dominant
CYP27A1	Apical Cortex	+++	Cerebrotendinous xanthomatosis, 213700 (3), Autosomal recessive
DIS3L2	Cytosol	+	Perlman syndrome, 267000 (3), Autosomal recessive
DLX3	Nucleus	++	Amelogenesis imperfecta, type IV, 104510 (3), Autosomal dominant; Trichodontoosseous syndrome, 190320 (3), Autosomal dominant
ELMOD3	Basal Body	+++	?Deafness, autosomal recessive 88, 615429 (3), Autosomal recessive
FAM161A	Nucleus & Microtubule	+++	Retinitis pigmentosa 28, 606068 (3)
FLNA	Cytosol	+++	Cardiac valvular dysplasia, X-linked, 314400 (3), X-linked recessive;

			Congenital short bowel syndrome, 300048 (3), X-linked recessive; FG syndrome 2, 300321 (3); Frontometaphyseal dysplasia 1, 305620 (3), X-linked recessive; Heterotopia, periventricular, 300049 (3), X-linked dominant; Intestinal pseudoobstruction, neuronal, 300048 (3), X-linked recessive; Melnick-Needles syndrome, 309350 (3), X-linked dominant; Otopalatodigital syndrome, type I, 311300 (3), X-linked dominant; Otopalatodigital syndrome, type II, 304120 (3), X-linked dominant; Terminal osseous dysplasia, 300244 (3)
GORAB	Foci in cytosol_Trafficing foci	++	Geroderma osteodysplasticum, 231070 (3), Autosomal recessive
IFT140	Axoneme	+	Short-rib thoracic dysplasia 9 with or without polydactyly, 266920 (3), Autosomal recessive
KIF1C	ER	++	Spastic ataxia 2, autosomal recessive, 611302 (3), Autosomal recessive
KIF22	Nucleus	+	Spondyloepimetaphyseal dysplasia with joint laxity, type 2, 603546 (3), Autosomal dominant
LMNA	Nucleus	+++	Cardiomyopathy, dilated, 1A, 115200 (3), Autosomal dominant; Charcot-Marie-Tooth disease, type 2B1, 605588 (3), Autosomal recessive; Emery-Dreifuss muscular dystrophy 2, AD, 181350 (3), Autosomal dominant; Emery-Dreifuss muscular dystrophy 3, AR, 616516 (3), Autosomal recessive; Heart-hand syndrome, Slovenian type, 610140 (3), Autosomal dominant; Hutchinson-Gilford progeria, 176670 (3), Autosomal recessive, Autosomal dominant; Lipodystrophy, familial partial, type 2, 151660 (3), Autosomal dominant;

			Malouf syndrome, 212112 (3), Autosomal dominant; Mandibuloacral dysplasia, 248370 (3), Autosomal recessive; Muscular dystrophy, congenital, 613205 (3), Autosomal dominant; Muscular dystrophy, limb-girdle, type 1B, 159001 (3), Autosomal dominant; Restrictive dermopathy, lethal, 275210 (3), Autosomal recessive
LRTOMT	Axoneme & Fiber in cytosol	+++	Deafness, autosomal recessive 63, 611451 (3), Autosomal recessive
NEXN	Apical Cortex	+++	Cardiomyopathy, dilated, 1CC, 613122 (3); Cardiomyopathy, hypertrophic, 20, 613876 (3), Autosomal dominant
NOTCH2	ER	+++	Alagille syndrome 2, 610205 (3), Autosomal dominant; Hajdu-Cheney syndrome, 102500 (3), Autosomal dominant
PALLD	Apical Cortex	+++	{Pancreatic cancer, susceptibility to, 1}, 606856 (3)
PLS3	Apical Cortex	+++	Bone mineral density QTL18, osteoporosis
PKP2	Basal Body & Junction & Axoneme	+++	Arrhythmogenic right ventricular dysplasia 9, 609040 (3), Autosomal dominant
PLOD3	ER	++	Lysyl hydroxylase 3 deficiency, 612394 (3), Autosomal recessive
RAB28	Everywhere	+++	Cone-rod dystrophy 18, 615374 (3), Autosomal recessive
RSPH3	Axoneme & Nucleus	++	Ciliary dyskinesia, primary, 32, 616481 (3), Autosomal recessive
SH3GL1	Apical Cortex&Junction	+++	Leukemia, acute myeloid, 601626 (1), Autosomal dominant
SLC22A5	ER	+++	Carnitine deficiency, systemic primary, 212140 (3), Autosomal recessive
SLC4A1	ER	+++	[Blood group, Diego], 110500 (3); [Blood group, Froese], 601551 (3); [Blood group, Swann], 601550 (3); [Blood group, Waldner], 112010 (3);

			[Blood group, Wright], 112050 (3); Cryohydrocytosis, 185020 (3), Autosomal dominant; [Malaria, resistance to], 611162 (3); Ovalocytosis, SA type, 166900 (3), Autosomal dominant; Renal tubular acidosis, distal, AD, 179800 (3), Autosomal dominant; Renal tubular acidosis, distal, AR, 611590 (3), Autosomal recessive; Spherocytosis, type 4, 612653 (3), Autosomal dominant
SPARC	ER & Apical Cortex	+++	Osteogenesis imperfecta, type XVII, 616507 (3), Autosomal recessive
SPECC1L	others_fibers	++	?Facial clefting, oblique, 1, 600251 (3), Isolated cases; Opitz GBBB syndrome, type II, 145410 (3), Autosomal dominant
SPEG	Everywhere	+	Centronuclear myopathy 5, 615959 (3), Autosomal recessive
SPRED1	others_Basolateral Membrane & Foci	+++	Legius syndrome, 611431 (3), Autosomal dominant
TCTN3	Basal Body & Foci in cytosol	++	Joubert syndrome 18, 614815 (3), Autosomal recessive; Orofaciodigital syndrome IV, 258860 (3), Autosomal recessive
TFAP2A	Cytosol	+++	Branchiooculofacial syndrome, 113620 (3), Autosomal dominant
TMEM38B	ER	+++	Osteogenesis imperfecta, type XIV, 615066 (3)
TPRN	Nucleus	+++	Deafness, autosomal recessive 79, 613307 (3), Autosomal recessive
TRIM37	Basal Body & Junction	++	Mulibrey nanism, 253250 (3), Autosomal recessive
TTC7A	Basal Body & Cytosol	++	Gastrointestinal defects and immunodeficiency syndrome, 243150 (3), Autosomal recessive
UQCRQ	Cytosol	+++	Mitochondrial complex III deficiency, nuclear type 4, 615159 (3), Autosomal recessive
WDR60	Basal Body	+++	Short-rib thoracic dysplasia 8 with or without polydactyly, 615503 (3),

			Autosomal recessive

Table B2 The screened genes with OMIM annotation

Appendix C Knock out and knock down verification

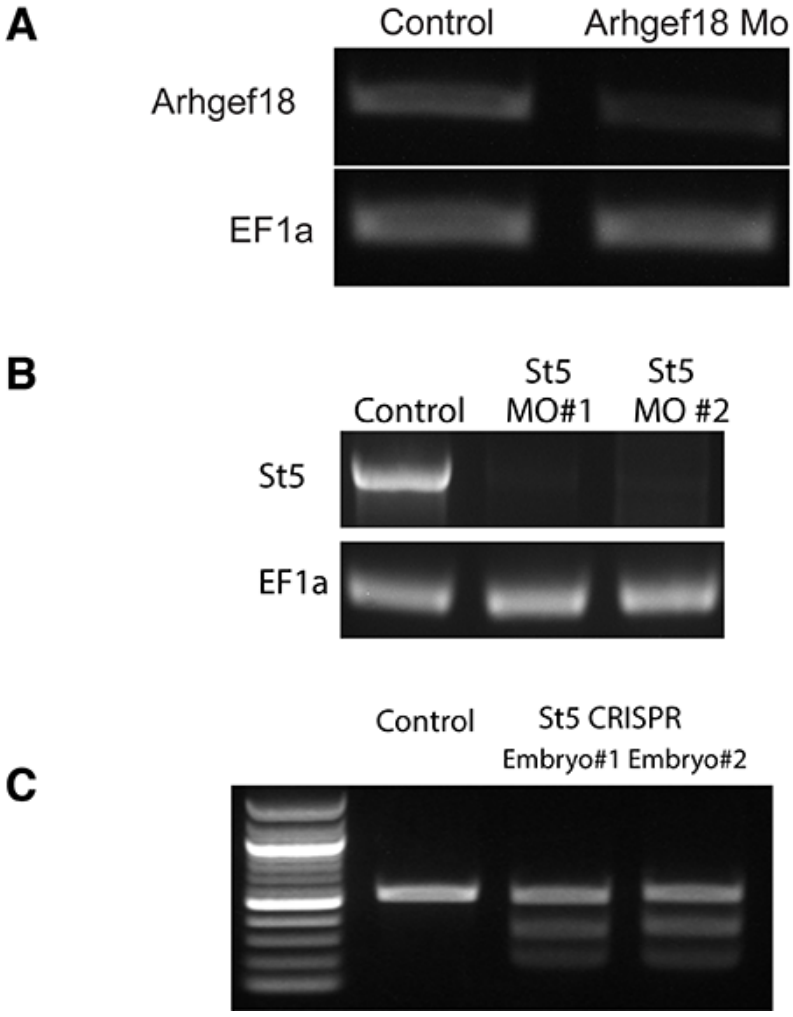

Figure C.1 The verifications of Morhpolino knocknockdownown and CRIPR knockout

(A) The level of Arhgef18 was efficiently reduced by Arhgef10 antisense nucleotides. The level of Arhgef18 was decreased by 71% in Arhgef18 knockdown compared to controls. EF1a, a reference gene. **(B)** The level of Dennd2b was significantly reduced by injections of Dennd2b antisense nucleotides. The transcript level of Dennd2b was decreased to 26% and 23%, respectively compared to controls. EF1a, a reference gene. **(C)** T7 Endonuclease I (T7EI) assay showed Dennd2b CRISPR induced genomic mutation in Dennd2b

Reference

1. Brooks, E.R. & Wallingford, J.B. Multiciliated cells. *Current Biology* **24**, R973-R982 (2014).
2. Afzelius, B. Cilia‐related diseases. *The Journal of pathology* **204**, 470-477 (2004).
3. Lyons, R., Saridogan, E. & Djahanbakhch, O. The reproductive significance of human Fallopian tube cilia. *Human reproduction update* **12**, 363-372 (2006).
4. Antunes, M.B. & Cohen, N.A. Mucociliary clearance–a critical upper airway host defense mechanism and methods of assessment. *Current opinion in allergy and clinical immunology* **7**, 5-10 (2007).
5. Del Bigio, M.R. Ependymal cells: biology and pathology. *Acta neuropathologica* **119**, 55-73 (2010).
6. Shah, A.S., Ben-Shahar, Y., Moninger, T.O., Kline, J.N. & Welsh, M.J. Motile cilia of human airway epithelia are chemosensory. *Science* **325**, 1131-1134 (2009).
7. Choksi, S.P., Lauter, G., Swoboda, P. & Roy, S. Switching on cilia: transcriptional networks regulating ciliogenesis. *Development* **141**, 1427-1441 (2014).
8. Spassky, N. & Meunier, A. The development and functions of multiciliated epithelia. *Nature Reviews Molecular Cell Biology* **18**, 423-436 (2017).
9. Deblandre, G.A., Wettstein, D.A., Koyano-Nakagawa, N. & Kintner, C. A two-step mechanism generates the spacing pattern of the ciliated cells in the skin of *Xenopus* embryos. *Development* **126**, 4715-4728 (1999).
10. Lafkas, D. et al. Therapeutic antibodies reveal Notch control of transdifferentiation in the adult lung. *Nature* **528**, 127 (2015).
11. Tsao, P.-N. et al. Notch signaling controls the balance of ciliated and secretory cell fates in developing airways. *Development* **136**, 2297-2307 (2009).
12. Marcet, B. et al. Control of vertebrate multiciliogenesis by miR-449 through direct repression of the Delta/Notch pathway. *Nature cell biology* **13**, 694 (2011).
13. Cibois, M. et al. BMP signaling controls the construction of vertebrate mucociliary epithelia. *Development* **142**, 2352-2363 (2015).
14. Huang, Y.-L. & Niehrs, C. Polarized Wnt signaling regulates ectodermal cell fate in *Xenopus*. *Developmental cell* **29**, 250-257 (2014).
15. Zhou, F. et al. Gmnc is a master regulator of the multiciliated cell differentiation program. *Current Biology* **25**, 3267-3273 (2015).
16. Arbi, M. et al. GemC1 controls multiciliogenesis in the airway epithelium. *EMBO reports* **17**, 400-413 (2016).
17. Terré, B. et al. GEMC1 is a critical regulator of multiciliated cell differentiation. *The EMBO journal* **35**, 942-960 (2016).
18. Stubbs, J.L., Oishi, I., Belmonte, J.C.I. & Kintner, C. The forkhead protein Foxj1 specifies node-like cilia in *Xenopus* and zebrafish embryos. *Nature genetics* **40**, 1454-1460 (2008).

19. Yu, X., Ng, C.P., Habacher, H. & Roy, S. Foxj1 transcription factors are master regulators of the motile ciliogenic program. *Nature genetics* **40**, 1445-1453 (2008).
20. Choksi, S.P., Babu, D., Lau, D., Yu, X. & Roy, S. Systematic discovery of novel ciliary genes through functional genomics in the zebrafish. *Development* **141**, 3410-3419 (2014).
21. Stubbs, J., Vladar, E., Axelrod, J. & Kintner, C. Multicilin promotes centriole assembly and ciliogenesis during multiciliate cell differentiation. *Nature cell biology* **14**, 140 (2012).
22. Ma, L., Quigley, I., Omran, H. & Kintner, C. Multicilin drives centriole biogenesis via E2f proteins. *Genes & development* **28**, 1461-1471 (2014).
23. El Zein, L. et al. RFX3 governs growth and beating efficiency of motile cilia in mouse and controls the expression of genes involved in human ciliopathies. *J Cell Sci* **122**, 3180-3189 (2009).
24. Chung, M.-I. et al. RFX2 is broadly required for ciliogenesis during vertebrate development. *Developmental biology* **363**, 155-165 (2012).
25. Chung, M.-I. et al. Coordinated genomic control of ciliogenesis and cell movement by RFX2. *Elife* **3**, e01439 (2014).
26. Quigley, I.K. & Kintner, C. Rfx2 stabilizes Foxj1 binding at chromatin loops to enable multiciliated cell gene expression. *PLoS genetics* **13**, e1006538 (2017).
27. Stubbs, J.L., Davidson, L., Keller, R. & Kintner, C. Radial intercalation of ciliated cells during *Xenopus* skin development. *Development* **133**, 2507-2515 (2006).
28. Walck-Shannon, E. & Hardin, J. Cell intercalation from top to bottom. *Nature reviews. Molecular cell biology* **15**, 34 (2014).
29. Dubaissi, E. & Papalopulu, N. Embryonic frog epidermis: a model for the study of cell-cell interactions in the development of mucociliary disease. *Disease models & mechanisms* **4**, 179-192 (2011).
30. Sirour, C. et al. Dystroglycan is involved in skin morphogenesis downstream of the Notch signaling pathway. *Molecular biology of the cell* **22**, 2957-2969 (2011).
31. Kim, K., Lake, B.B., Haremaki, T., Weinstein, D.C. & Sokol, S.Y. Rab11 regulates planar polarity and migratory behavior of multiciliated cells in *Xenopus* embryonic epidermis. *Developmental Dynamics* **241**, 1385-1395 (2012).
32. Werner, M.E. et al. Radial intercalation is regulated by the Par complex and the microtubule-stabilizing protein CLAMP/Spef1. *J Cell Biol* **206**, 367-376 (2014).
33. Ossipova, O. et al. The involvement of PCP proteins in radial cell intercalations during Xenopus embryonic development. *Developmental biology* **408**, 316-327 (2015).
34. Sedzinski, J., Hannezo, E., Tu, F., Biro, M. & Wallingford, J.B. Emergence of an apical epithelial cell surface in vivo. *Developmental cell* **36**, 24-35 (2016).
35. Nachury, M.V., Seeley, E.S. & Jin, H. Trafficking to the ciliary membrane: how to get across the periciliary diffusion barrier? *Annual review of cell and developmental biology* **26**, 59-87 (2010).
36. Yang, T.T. et al. Superresolution pattern recognition reveals the architectural map of the ciliary transition zone. *Scientific reports* **5**, 14096 (2015).

37. Tanos, B.E. et al. Centriole distal appendages promote membrane docking, leading to cilia initiation. *Genes & development* **27**, 163-168 (2013).
38. Humbert, M.C. et al. ARL13B, PDE6D, and CEP164 form a functional network for INPP5E ciliary targeting. *Proceedings of the National Academy of Sciences* **109**, 19691-19696 (2012).
39. Wei, Q. et al. Transition fibre protein FBF1 is required for the ciliary entry of assembled intraflagellar transport complexes. *Nature communications* **4**, 2750 (2013).
40. Park, T.J., Mitchell, B.J., Abitua, P.B., Kintner, C. & Wallingford, J.B. Dishevelled controls apical docking and planar polarization of basal bodies in ciliated epithelial cells. *Nature genetics* **40**, 871-879 (2008).
41. Butler, M.T. & Wallingford, J.B. Control of vertebrate core planar cell polarity protein localization and dynamics by Prickle 2. *Development* **142**, 3429-3439 (2015).
42. Jaffe, K.M. et al. c21orf59/kurly controls both cilia motility and polarization. *Cell reports* **14**, 1841-1849 (2016).
43. Vladar, E.K., Bayly, R.D., Sangoram, A.M., Scott, M.P. & Axelrod, J.D. Microtubules enable the planar cell polarity of airway cilia. *Current Biology* **22**, 2203-2212 (2012).
44. Werner, M.E. et al. Actin and microtubules drive differential aspects of planar cell polarity in multiciliated cells. *J Cell Biol* **195**, 19-26 (2011).
45. Kunimoto, K. et al. Coordinated ciliary beating requires Odf2-mediated polarization of basal bodies via basal feet. *Cell* **148**, 189-200 (2012).
46. Turk, E. et al. Zeta-tubulin is a member of a conserved tubulin module and is a component of the centriolar basal foot in multiciliated cells. *Current Biology* **25**, 2177-2183 (2015).
47. Dehring, D.A.K. et al. Deuterosome-mediated centriole biogenesis. *Developmental cell* **27**, 103-112 (2013).
48. Klotz, C., Bordes, N., Laine, M.-C., Sandoz, D. & Bornens, M. Myosin at the apical pole of ciliated epithelial cells as revealed by a monoclonal antibody. *The Journal of cell biology* **103**, 613-619 (1986).
49. Lemullois, M., Boisvieux-Ulrich, E., Laine, M.-C., Chailley, B. & Sandoz, D. Development and functions of the cytoskeleton during ciliogenesis in metazoa. *Biology of the Cell* **63**, 195-208 (1988).
50. Pan, J., You, Y., Huang, T. & Brody, S.L. RhoA-mediated apical actin enrichment is required for ciliogenesis and promoted by Foxj1. *Journal of cell science* **120**, 1868-1876 (2007).
51. Antoniades, I., Stylianou, P. & Skourides, P.A. Making the connection: ciliary adhesion complexes anchor basal bodies to the actin cytoskeleton. *Developmental cell* **28**, 70-80 (2014).
52. Ioannou, A., Santama, N. & Skourides, P.A. Xenopus laevis nucleotide binding protein 1 (xNubp1) is important for convergent extension movements and controls

ciliogenesis via regulation of the actin cytoskeleton. *Developmental biology* **380**, 243-258 (2013).
53. Eguether, T. et al. The deubiquitinating enzyme CYLD controls apical docking of basal bodies in ciliated epithelial cells. *Nature communications* **5** (2014).
54. Epting, D. et al. The Rac1 regulator ELMO controls basal body migration and docking in multiciliated cells through interaction with Ezrin. *Development* **142**, 174-184 (2015).
55. Yasunaga, T. et al. The polarity protein Inturned links NPHP4 to Daam1 to control the subapical actin network in multiciliated cells. *J Cell Biol* **211**, 963-973 (2015).
56. Gegg, M. et al. Flattop regulates basal body docking and positioning in mono-and multiciliated cells. *Elife* **3**, e03842 (2014).
57. Burke, M.C. et al. Chibby promotes ciliary vesicle formation and basal body docking during airway cell differentiation. *J Cell Biol* **207**, 123-137 (2014).
58. Li, F.-Q. et al. BAR Domain-Containing FAM92 Proteins Interact with Chibby1 To Facilitate Ciliogenesis. *Molecular and Cellular Biology* **36**, 2668-2680 (2016).
59. Sandoz, D. et al. Organization and functions of cytoskeleton in metazoan ciliated cells. *Biology of the Cell* **63**, 183-193 (1988).
60. Chailley, B., Frappier, T., Regnouf, F. & Laine, M. Immunological detection of spectrin during differentiation and in mature ciliated cells from quail oviduct. *Journal of cell science* **93**, 683-690 (1989).
61. Chailley, B., Nicolas, G. & Lainé, M.-C. Organization of actin microfilaments in the apical border of oviduct ciliated cells. *Biology of the Cell* **67**, 81-90 (1989).
62. Avasthi, P. et al. Actin is required for IFT regulation in Chlamydomonas reinhardtii. *Current Biology* **24**, 2025-2032 (2014).
63. Kim, J. et al. Actin remodelling factors control ciliogenesis by regulating YAP/TAZ activity and vesicle trafficking. *Nature communications* **6**, 6781 (2015).
64. Kim, J. et al. Functional genomic screen for modulators of ciliogenesis and cilium length. *Nature* **464**, 1048 (2010).
65. Kohli, P. et al. The ciliary membrane‐associated proteome reveals actin‐binding proteins as key components of cilia. *EMBO reports*, e201643846 (2017).
66. Chen, Z., Indjeian, V.B., McManus, M., Wang, L. & Dynlacht, B.D. CP110, a cell cycle-dependent CDK substrate, regulates centrosome duplication in human cells. *Developmental cell* **3**, 339-350 (2002).
67. Spektor, A., Tsang, W.Y., Khoo, D. & Dynlacht, B.D. Cep97 and CP110 suppress a cilia assembly program. *Cell* **130**, 678-690 (2007).
68. Tsang, W.Y. et al. CP110 suppresses primary cilia formation through its interaction with CEP290, a protein deficient in human ciliary disease. *Developmental cell* **15**, 187-197 (2008).
69. Tsang, W.Y. & Dynlacht, B.D. CP110 and its network of partners coordinately regulate cilia assembly. *Cilia* **2**, 9 (2013).

70. Kobayashi, T., Tsang, W.Y., Li, J., Lane, W. & Dynlacht, B.D. Centriolar kinesin Kif24 interacts with CP110 to remodel microtubules and regulate ciliogenesis. *Cell* **145**, 914-925 (2011).
71. Goetz, S.C., Liem, K.F. & Anderson, K.V. The spinocerebellar ataxia-associated gene Tau tubulin kinase 2 controls the initiation of ciliogenesis. *Cell* **151**, 847-858 (2012).
72. Li, J. et al. USP33 regulates centrosome biogenesis via de-ubiquitylation of a centriolar protein, CP110. *Nature* **495** (2013).
73. Song, R. et al. miR-34/449 miRNAs are required for motile ciliogenesis by repressing cp110. *Nature* **510**, 115 (2014).
74. Yadav, S.P. et al. Centrosomal protein CP110 controls maturation of the mother centriole during cilia biogenesis. *Development* **143**, 1491-1501 (2016).
75. Walentek, P. et al. Ciliary transcription factors and miRNAs precisely regulate Cp110 levels required for ciliary adhesions and ciliogenesis. *Elife* **5** (2016).
76. Lai, C.K. et al. Functional characterization of putative cilia genes by high-content analysis. *Molecular biology of the cell* **22**, 1104-1119 (2011).
77. Gupta, G.D. et al. A dynamic protein interaction landscape of the human centrosome-cilium interface. *Cell* **163**, 1484-1499 (2015).
78. Wheway, G. et al. An siRNA-based functional genomics screen for the identification of regulators of ciliogenesis and ciliopathy genes. *Nature cell biology* **17**, 1074 (2015).
79. Boldt, K. et al. An organelle-specific protein landscape identifies novel diseases and molecular mechanisms. *Nature communications* **7**, 11491 (2016).
80. Kim, J.H. et al. Genome-wide screen identifies novel machineries required for both ciliogenesis and cell cycle arrest upon serum starvation. *Biochimica et Biophysica Acta (BBA)-Molecular Cell Research* **1863**, 1307-1318 (2016).
81. Balestra, F.R., Strnad, P., Flückiger, I. & Gönczy, P. Discovering regulators of centriole biogenesis through siRNA-based functional genomics in human cells. *Developmental cell* **25**, 555-571 (2013).
82. Austin-Tse, C. et al. Zebrafish ciliopathy screen plus human mutational analysis identifies C21orf59 and CCDC65 defects as causing primary ciliary dyskinesia. *The American Journal of Human Genetics* **93**, 672-686 (2013).
83. Hoh, R.A., Stowe, T.R., Turk, E. & Stearns, T. Transcriptional program of ciliated epithelial cells reveals new cilium and centrosome components and links to human disease. *PloS one* **7**, e52166 (2012).
84. Jensen, V.L. et al. Whole-Organism Developmental Expression Profiling Identifies RAB-28 as a Novel Ciliary GTPase Associated with the BBSome and Intraflagellar Transport. *PLoS genetics* **12**, e1006469 (2016).
85. Hayes, J.M. et al. Identification of novel ciliogenesis factors using a new in vivo model for mucociliary epithelial development. *Developmental biology* **312**, 115-130 (2007).

86. Stauber, M. et al. Identification of FOXJ1 effectors during ciliogenesis in the foetal respiratory epithelium and embryonic left-right organiser of the mouse. *Developmental biology* **423**, 170-188 (2017).
87. Horvath, G.C., Kistler, W.S. & Kistler, M.K. RFX2 is a potential transcriptional regulatory factor for histone H1t and other genes expressed during the meiotic phase of spermatogenesis. *Biology of reproduction* **71**, 1551-1559 (2004).
88. Boutros, M., Heigwer, F. & Laufer, C. Microscopy-based high-content screening. *Cell* **163**, 1314-1325 (2015).
89. Horani, A. et al. CCDC65 mutation causes primary ciliary dyskinesia with normal ultrastructure and hyperkinetic cilia. *PloS one* **8**, e72299 (2013).
90. Delmaghani, S. et al. Mutations in CDC14A, encoding a protein phosphatase involved in hair cell ciliogenesis, cause autosomal-recessive severe to profound deafness. *The American Journal of Human Genetics* **98**, 1266-1270 (2016).
91. Ahmed, Z.M. et al. Mutations of LRTOMT, a fusion gene with alternative reading frames, cause nonsyndromic deafness in humans. *Nature genetics* **40**, 1335-1340 (2008).
92. Li, Y. et al. Mutations in TPRN cause a progressive form of autosomal-recessive nonsyndromic hearing loss. *The American Journal of Human Genetics* **86**, 479-484 (2010).
93. van den Ouweland, A.M. et al. Mutations in the vasopressin type 2 receptor gene (AVPR2) associated with nephrogenic diabetes insipidus. *Nature genetics* **2**, 99-102 (1992).
94. Tateishi, K., Nishida, T., Inoue, K. & Tsukita, S. Three-dimensional Organization of Layered Apical Cytoskeletal Networks Associated with Mouse Airway Tissue Development. *Scientific Reports* **7** (2017).
95. Mercey, O., Kodjabachian, L., Barbry, P. & Marcet, B. MicroRNAs as key regulators of GTPase-mediated apical actin reorganization in multiciliated epithelia. *Small GTPases* **7**, 54-58 (2016).
96. Ioannou, M.S. et al. DENND2B activates Rab13 at the leading edge of migrating cells and promotes metastatic behavior. *J Cell Biol* **208**, 629-648 (2015).
97. Kleczkowska, A., Fryns, J., Jaeken, J. & Van den Berghe, H. in Annales de genetique 126-128 (1988).
98. Göhring, I. et al. Disruption of ST5 is associated with mental retardation and multiple congenital anomalies. *Journal of medical genetics* **47**, 91-98 (2010).
99. Taschner, M. & Lorentzen, E. The intraflagellar transport machinery. *Cold Spring Harbor perspectives in biology* **8**, a028092 (2016).
100. Čajánek, L. & Nigg, E.A. Cep164 triggers ciliogenesis by recruiting Tau tubulin kinase 2 to the mother centriole. *Proceedings of the National Academy of Sciences* **111**, E2841-E2850 (2014).
101. Garcia-Gonzalo, F.R. & Reiter, J.F. Open sesame: how transition fibers and the transition zone control ciliary composition. *Cold Spring Harbor perspectives in biology* **9**, a028134 (2017).

102. Brusse, E. et al. Spinocerebellar ataxia associated with a mutation in the fibroblast growth factor 14 gene (SCA27): A new phenotype. *Movement disorders* **21**, 396-401 (2006).
103. Drew, K. et al. Integration of over 9,000 mass spectrometry experiments builds a global map of human protein complexes. *Molecular Systems Biology* **13** (2017).
104. Cao, J. et al. miR-129-3p controls cilia assembly by regulating CP110 and actin dynamics. *Nature cell biology* **14**, 697 (2012).
105. Assis, L. et al. The molecular motor Myosin Va interacts with the cilia-centrosomal protein RPGRIP1L. *Scientific Reports* **7** (2017).
106. Wang, W.-J. et al. CEP162 is an axoneme-recognition protein promoting ciliary transition zone assembly at the cilia base. *Nature cell biology* **15**, 591 (2013).
107. Herawati, E. et al. Multiciliated cell basal bodies align in stereotypical patterns coordinated by the apical cytoskeleton. *J Cell Biol* **214**, 571-586 (2016).
108. Chung, M.I. et al. Coordinated genomic control of ciliogenesis and cell movement by RFX2. *Elife* **3**, e01439 (2014).
109. Stubbs, J.L., Davidson, L., Keller, R. & Kintner, C. Radial intercalation of ciliated cells during Xenopus skin development. *Development* **133**, 2507-15 (2006).
110. Vize, P.D., Melton, D.A., Hemmati-Brivanlou, A. & Harland, R.M. Assays for gene function in developing Xenopus embryos. *Methods Cell Biol* **36**, 367-87 (1991).
111. Nieuwkoop, P.D. & Faber, J. Normal Table of Xenopus laevis. (Garland New York, 1967).
112. Rual, J.F. et al. Towards a proteome-scale map of the human protein-protein interaction network. *Nature* **437**, 1173-8 (2005).
113. Team, M.G.C.P. et al. The completion of the Mammalian Gene Collection (MGC). *Genome Res* **19**, 2324-33 (2009).
114. Kieserman, E.K., Lee, C., Gray, R.S., Park, T.J. & Wallingford, J.B. High-magnification in vivo imaging of Xenopus embryos for cell and developmental biology. *Cold Spring Harb Protoc* **2010**, pdb prot5427 (2010).
115. Sive, H.L., Grainger, R.M. & Harland, R.M. Early Development of Xenopus laevis: A Laboratory Manual. (2000).

Vita

Fan Tu was born in Xiaogan, China. After graduating from Wanzhou Number 2 Middle School in 2005, he went to Beijing Normal University. In 2009, he received Bachelor of Science degree in Biology. In 2011 he entered the Ph.D. program for Cellular and Molecular Biology at the University of Texas at Austin.